공학석사 학위논문

Enhancement and Optimization on Cooling Performance of Gas-based Fusion Reactor Blanket using Binary and Ternary Gas Mixtures

혼합 기체를 이용한 기체 기반 핵융합로 블랭킷 냉각 성능 증진 및 최적화

2013 년 8 월

서울대학교 대학원

에너지시스템공학부

박 일 웅

Enhancement and Optimization on Cooling Performance of Gas-based Fusion Reactor Blanket using Binary and Ternary Gas Mixtures

혼합기체를 이용한 기체 기반 핵융합로 블랭킷 냉각 성능 증진 및 최적화

지도교수 조 형 규

이 논문을 공학석사 학위논문으로 제출함
2013 년 7 월

서울대학교 대학원
에너지시스템공학부
박 일 웅

박일웅의 석사 학위논문을 인준함
2013 년 7 월

위 원 장 김 응 수 (인)

부위원장 조 형 규 (인)

위 원 박 군 철 (인)

Abstract

Enhancement and Optimization on Cooling Performance of Gas-based Fusion Reactor Blanket using Binary and Ternary Gas Mixtures

Il-Woong Park

Department of Energy System Engineering

The Graduate School

Seoul National University

Several coolants are considered as candidates of the fusion blanket coolant, and among those, helium is considered as the most viable option. As a coolant, helium does have drawbacks on the cooling performance, but at the same time it has certain advantages in the safety aspects when compared to other coolants which are considered for the cooling of fusion blanket. The gas mixture concept based on helium gas, in order to retain the benefits in safety aspects of helium and also to improve the heat transfer performance, is proposed in this study.

The correlation is developed for scaled velocity and pumping power with maintaining the same thermal performance. To be specific, scaled velocity and pumping power were composed of four fluid properties and two overall

geometrical parameters. And the Dittus-Boelter correlation for heat transfer coefficient and Blasius correlation for friction factor are used for developing the correlation. The developed correlation has the form of Figure-of-merit (FOM) that is a quantity used to characterize the performance simply. Consequently, the purpose of the developed correlation is to compare the heat transfer performance of various gases before conducting the detailed analysis for nuclear fusion blanket.

Evaluation on heat transfer performance has been conducted for binary and ternary gas mixtures. For evaluation, we select carbon dioxide, argon, neon, krypton, xenon, and nitrogen as gases that are to be mixed with helium. Cooling capacity of binary gas mixtures are compared to that of ternary gas mixtures. The results show that the mixture gas improves cooling capability compared to pure gas. Based on the evaluation, the gas mixture concept which has better heat transfer capacity and also safety due to low operating pressure is proposed. It was noted, evaluation results show that ternary mixture gases show no further improvement compared to binary mixture in heat transfer performance.

The correlation developed in this study was validated through Computational Fluid Dynamics (CFD) simulation. Validation model used TER HCML TBM Blanket (International Thermonuclear Experimental Reactor Helium Cooled Molten Lithium Test Blanket Module) which utilizes helium coolant (300 ℃ and 8 MPa). Helium and carbon dioxide mixture is used for validation case, and the validation results demonstrate that the calculation results of the developed correlation are in good agreement with the calculation data obtained using CFD code. Furthermore, the Reynolds number and Prandtl number are considered for improving the developed correlation based on validation results. The correlation is modified using the Kays and Crawfold correlation. Moreover, the error analysis

for scaled pumping power is conducted based on the error of a heat transfer coefficient.

Keywords

Gas-based fusion reactor, Fusion blanket coolant, Gas mixtures, Figure-of-Merit (FOM), Scaling correlation, CFD, ITER HCML TBM

Student Number: 2011-23422

List of Contents

List of Tables

List of Figures

Chapter 1

Introduction

1.1 Background and Motivation

Korean fusion research and development have strategy consisting of several major programs. The strategy is made up of the K-STAR (Korea Superconducting Tokamak Advanced Research; Lee et al., 2001), the ITER (International Thermonuclear Experimental Reactor; Tomabechi et al., 1991), the K-DEMO (Korean DEMO Reactor; Kim et al., 2013) and a commercial fusion reactor. The KSTAR program heads for a long-pulse advanced tokamak operation. The ITER project will conduct the burning plasma experiment and has the objective to test the concept for tritium breeding relevant with power generation. The K-DEMO will demonstrate the production of net electricity from a fusion reactor. (Lee et al., 2007) And the Korean fusion development strategy is illustrated as Fig. 1.1.

The blanket is one of the key components in the nuclear fusion reactor. It has two main engineering goals which are very relevant with object of ITER and K-DEMO project. One of them is the tritium self-sufficiency. For that, demonstration of the tritium breeding capability is needed, and the tritium breeding concept is illustrated in Fig. 1.2. And another main engineering goal is producing electricity. For electricity production, the blanket needs to convert the

neutron energy generated by fusion reactions into thermal energy.

In the aspects of two main goals of the blanket, thermal hydraulic analysis for fusion blanket is very important. The first reason is that the tritium breeding is occurred in suitable temperature distribution on breeder and multiplier. And another reason is that the coolant conditions of inlet and outlet region have a dominant effect on generating electricity. Moreover, one of the major thermal design restrictions of fusion blanket is the temperature windows of structural material. (Zinkle and Ghoniem, 2000) The minimum and maximum temperatures of structure material are constrained by them. Satisfying them is challenging because the surface heating from plasma and neutron heating inside blanket are large. Consequently, the cooling performance of coolant and thermal hydraulic analysis for blanket are important for blanket design in order to achieve the main goals of blanket and to overcome the design restriction of it.

Generally, many fusion reactor blankets have layered internal structures consisting of breeders, multipliers, reflectors, coolant channels, etc. Those characteristics of fusion blanket make possible to generalize the fusion blanket geometry. Temperature distribution is governed by thermal characteristics in the coolant layer. This concept which has general geometry enables to analyze blanket's thermal condition as useful state in this study.

Several coolants are considered as a fusion reactor coolant. Water and liquid metal have an advantage of the cooling performance. However, they have drawbacks on the safety. For example water and liquid metal have possibility to have chemical reactions in fusion facilities. (Piet et al., 1987) On the contrary, helium has an advantage of the safety. The helium is suitable for blanket coolant, because the safety issue of blanket coolant is rising. Nevertheless, helium has a

shortcoming on heat transfer capability. Thus, the gas mixture concept that retains merits of safety using helium coolant and obtains better cooling performance by mixing with other coolants is proposed for this study.

Heat transfer coefficient and pressure loss of the binary gas based on helium have been reported to suggest gas mixture for gas-cooled nuclear power plants (El-Genk et al., 2008). The results show that heat transfer coefficient of binary gas mixed with helium and xenon with specific condition is 7% higher than for that of helium.

On the contrary, this study focused on achieving the same heat transfer performance that is the major difference between previous studies which has focused on same molecular flow rate. To be specific, the fusion reactor characteristics are different with nuclear power plant characteristics. In the fusion, reactor has more severe limitation of the temperature window for structure material due to high energy of neutrons. Thus, in the point of achieving the same heat transfer, the analysis is conducted using velocity and pumping power instead of heat transfer coefficient enhancement.

Furthermore, the pumping power is considered as one of the major parts of analyzing the fusion reactor. Because the large pumping power due to using helium as a coolant, the fusion reactor has low efficiency for generating electricity. Thus, the gas mixture concept is motivated from those shortcomings. Consequently, in this study, thermal analysis for fusion blanket is conducted in aspect of pumping power for improving the cooling performance.

1.2 Objective and Scope

The objectives of this study are to develop the correlation for comparing the thermal performance of gas mixtures, to evaluate the cooling performance of various gas mixtures including binary and ternary gas mixtures, and to validate of thermal performance enhancement using CFD (Computational Fluids Dynamics) simulation. Based on the results, the concept of cooling fusion blanket using mixture gas is proposed in this study. The outline of this study is illustrated in Fig. 1.3. Feasibility is investigated and the details are explained below.

Development of Correlation: The objective is to develop the correlations which are scaled velocity and pumping power for maintaining the same thermal performance. Those correlations have form of FOM (Figure-of-Merit) which is easy to compare the heat transfer performance between several gases and gas mixtures. The correlations have the simple form composed by material properties of coolant and overall geometrical parameters. Dittus-Boelter correlation (Dittus and Boelter, 1930) which is widely applicable and Blasius correlation (Blasius et al., 1913) which is commonly accepted are used for development of correlation.

Evaluation on cooling performance: Evaluation on effectiveness of heat transfer enhancement is conducted by using the derived correlation. Binary gas mixtures and ternary gas mixtures are the target for the evaluation. Comparisons of cooling capacity for mixture gases are carried out. Furthermore, the mechanism for increasing heat transfer performance by

mixing gas is examined using sensitivity of material properties for FOM. Based on the evaluation, the mixture gas concept which has better cooling performance and has better safety due to low operating pressure than pure helium coolant is proposed.

Validation of developed correlation: Developed correlations are validated using CFX-13, which is one kind of CFD (Computational Fluid Dynamics) codes. Especially, the calculation is conducted based on the RANS (Reynolds Averaged Navier-Stokes) model and standard k-ε model which are mostly used for turbulence model. HCML TBM (Helium Cooled Molten Lithium Test Blanket Module; Lee et al., 2009) which is one of the candidates for the ITER TBM in Korea is selected as a validation model. The CFD simulations were carried out for the helium and carbon dioxide mixture cases.

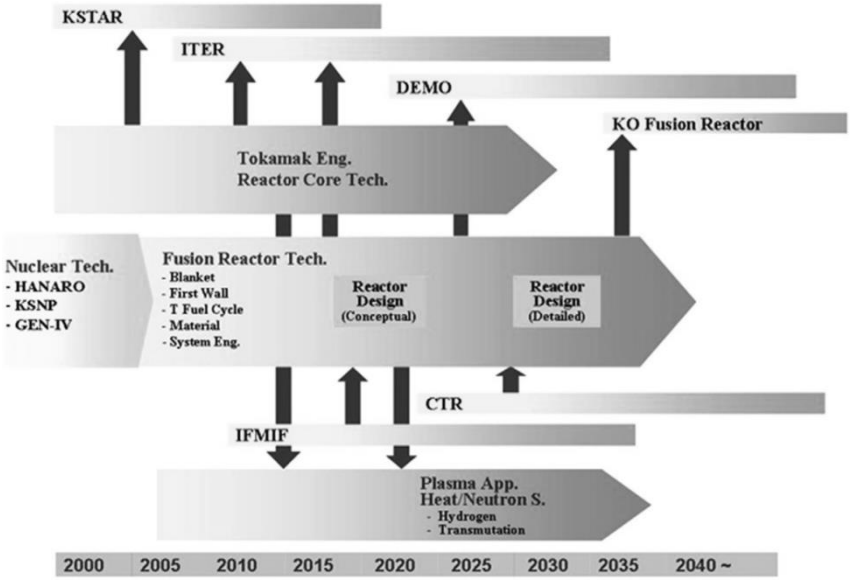

Figure 1.1 Korean fusion development strategies [Lee et al., 2007]

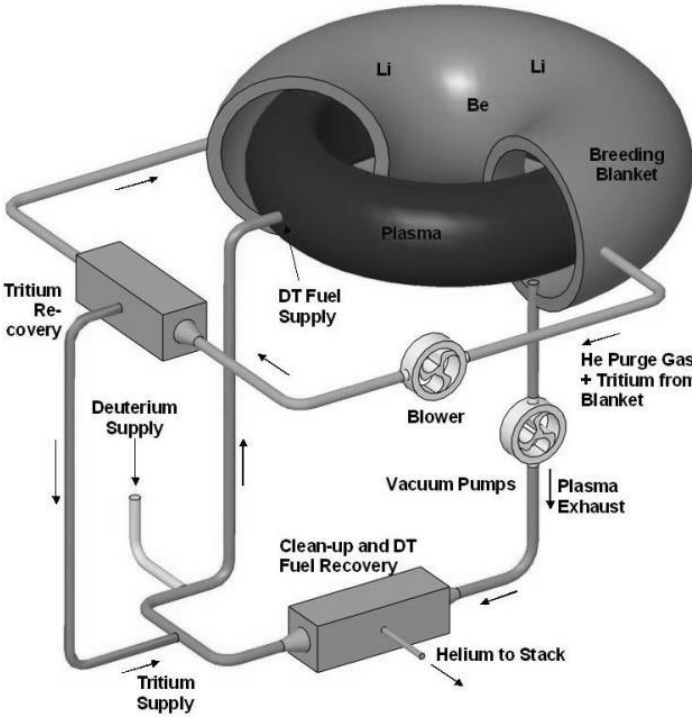

Figure 1.2 Tritium breeding concept of ITER [ITER., 1998]

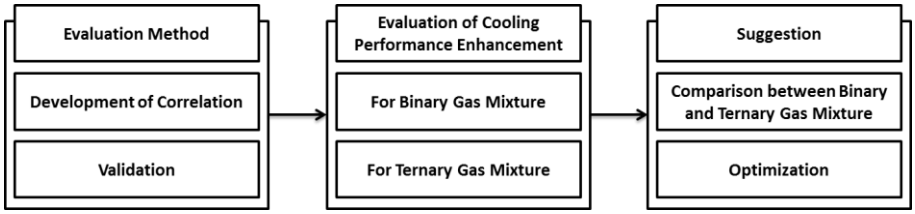

Figure 1.3 Outline of the study

Chapter 2

Development of Scaling Correlation for Comparisons on Gas Cooling Performance

In this chapter, the process for developing the scaling correlation is explained. This starts with the description of figure-of-merit (FOM) for cooling performance. This contains method to develop the correlation in detail. Moreover, the sensitivity of each material property for developed correlation is derived in this chapter.

2.1 Figure-of-Merit(FOM) for Cooling Performance

Figure-of-merit is the quantity that is used to characterize the performance in order to determine advantage for an application. It is established method for comparing the performance of device, system and method which is relative to its alternatives. The heat transfer capability of a system can be estimated and those of various systems can be compared with each other by accepting FOM. Because of the simple characteristic of figure-of-merit, it can be adopted to estimate the performance of system and compare the various cases for optimizing of the systems. Furthermore, the figure-of-merit has benefits reducing the effort for

analyzing the detail design.

Most of the proposed designs of solid type blanket in the fusion reactor have a similar concept that the coolant channels are stacked between the tritium breeders or neutron multipliers. The schematic diagram of solid blanket is depicted in Fig. 2.1. Therefore, if the heat transfer performance is same in the cooling channel, the temperature distribution and maximum temperature profile in the blanket can be estimated to be the same. Based on this approach, if we can compare the pumping powers of different coolants necessary to achieve the same cooling capability, it would be very beneficial to optimize the blanket thermal design and to analyze advantages and disadvantages of various coolants.

For this reason, this work attempts to develop a figure-of-merit to consider those purposes which are described previously. Figure-of-merit can represent heat transfer performance of the coolants. Derivation of a figure-of-merit in order to estimate relative pumping power is conducted in this study.

2.2 Derivation of Scaling Correlation

Derivation starts with heat transfer coefficient, the Reynolds number and the Prandtl number. By combining these equations, the velocity can be obtained. The Dittus-Boelter correlation is selected for heat transfer coefficient, and this can be expressed as:

$$h = \frac{k}{D_e} \cdot Nu = \frac{k}{D_e} \cdot \left(0.023 \,\mathrm{Re}^{0.8} \,\mathrm{Pr}^{0.4} \right). \tag{2.1}$$

And the Reynolds number and Prandtl number can be defined as:

$$\mathrm{Re} = \frac{\rho \cdot U \cdot D_e}{\mu}, \tag{2.2}$$

$$\mathrm{Pr} = \frac{C_p \cdot \mu}{k}. \tag{2.3}$$

By combining equation (2.1), (2.2) and (2.3) the heat transfer coefficient can be expressed by:

$$h = 0.023 \cdot (k)^{0.6} (\rho)^{0.8} (C_p)^{0.4} (\mu)^{-0.4} (D_e)^{-0.2} (U)^{0.8}. \tag{2.4}$$

Therefore, the flow velocity can be written by:

$$U = (111.65) \cdot (h)^{1.25} (k)^{-0.75} (\rho)^{-1} (C_p)^{-0.5} (\mu)^{0.5} (D_e)^{0.25}. \tag{2.5}$$

Constraints are that the volumetric heat removal rate should be maintained to achieve the same temperature distribution. The overall geometry and dimensions should be conserved for comparison. With these constraints, the following are considered that, for given total flow area, flow length and channel volume, the heat removal rate per unit temperature difference must be maintained as:

$$\dot{Q} = h \cdot A \cdot \Delta T / V, \tag{2.6}$$

$$D_e = \frac{4A_c}{P} = \frac{4V}{A}, \tag{2.7}$$

$$A = \frac{4 \cdot V_c}{D_e} = \frac{4 \cdot \alpha \cdot V}{D_e}. \tag{2.8}$$

Since this problem is assuming that the heat removal rate, volume, and temperature difference are maintained, the following is valid.

$$h \cdot A = \frac{\dot{Q} \cdot V}{\Delta T} = C_1 = const. \tag{2.9}$$

Therefore,

$$h = C_1\left(\frac{D_e}{4\cdot\alpha\cdot V}\right). \tag{2.10}$$

Inserting Eq.(2.10) into Eq.(2.5), velocity without the heat transfer coefficient term can be obtained as:

$$U = (111.65)\cdot\left(C_1\left(\frac{D_e}{4\cdot\alpha\cdot V}\right)\right)^{1.25}(k)^{-0.75}(\rho)^{-1}\left(C_p\right)^{-0.5}(\mu)^{0.5}\left(D_e\right)^{0.25}, \tag{2.11}$$

$$U \sim (k)^{-0.75}(\rho)^{-1}\left(C_p\right)^{-0.5}(\mu)^{0.5}\left(D_e\right)^{1.5}(\alpha)^{-1.25}. \tag{2.12}$$

Therefore, based on the Eq.(2.12), figure-of-merits for velocity for achieving the same heat transfer performance can be defined as follows.

$$\frac{U}{U_0} = FOM_U = \left(\frac{k}{k_0}\right)^{-0.75}\left(\frac{\rho}{\rho_0}\right)^{-1}\left(\frac{C_p}{C_{p0}}\right)^{-0.5}\left(\frac{\mu}{\mu_0}\right)^{0.5}\left(\frac{D_e}{D_{e0}}\right)^{1.5}\left(\frac{\alpha}{\alpha_0}\right)^{-1.25}. \tag{2.13}$$

And the figure-of-merits for the pumping powers can be derived by following procedure; Pumping power of the coolant can be expressed as:

$$P_{pump} = \frac{\Delta p\cdot G}{\eta}. \tag{2.14}$$

The cooling system is generally operated in the turbulent flow regime. Therefore, the frictional pressure drop is expressed by,

$$\Delta P = f\cdot\frac{1}{2}\rho\cdot U^2\cdot\frac{L}{D_e}. \tag{2.15}$$

The friction factor (f) can be calculated by Blasius formula for a smooth pipe as follows:

$$f = 0.316\cdot \mathrm{Re}^{-0.25} \tag{2.16}$$

The volumetric flow rate can be expressed by

$$G = U\cdot A_c = U\cdot\left(\frac{\alpha\cdot V}{L}\right). \tag{2.17}$$

Inserting Eqs. (2.13), (2.16), and (2.17) in Eq. (2.15), the following expression can be obtained as:

$$P_{pump} = \frac{\left(0.316 \cdot \left(\frac{\rho \cdot U \cdot D_e}{\mu} \right)^{-0.25} \cdot \frac{1}{2} \rho \cdot U^3 \cdot \left(\frac{\alpha}{D_e} \right) \cdot V \right)}{\eta}, \tag{2.18}$$

$$P_{pump} \sim \left\{ (k)^{-2.06} (\rho)^{-2.0} (C_p)^{-1.375} (\mu)^{1.625} \right\} \cdot \left\{ (D_e)^{2.875} (\alpha)^{-2.44} \right\}. \tag{2.19}$$

Therefore, based on the Eq.(2.19), figure-of-merits for velocity for achieving the same heat transfer performance can be defined as follows:

$$\frac{P_{pump}}{P_{pump0}} = FOM_P = \left\{ \left(\frac{k}{k_0} \right)^{-2.06} \left(\frac{\rho}{\rho_0} \right)^{-2.0} \left(\frac{C_p}{C_{p0}} \right)^{-1.375} \left(\frac{\mu}{\mu_0} \right)^{1.625} \right\} \cdot \left\{ \left(\frac{D_e}{D_{e0}} \right)^{2.875} \left(\frac{\alpha}{\alpha_0} \right)^{-2.44} \right\}. \tag{2.20}$$

2.3 Sensitivity of Scaling Correlation

Using the figure-of-merit developed previously, the sensitivity of each property for the figure-of-merit of velocity (FOM_U) can be calculated by normalized form as follows:

$$S_{U,k} = \frac{\partial FOM_U / FOM_U}{\partial k / k} = -0.75, \tag{2.21}$$

$$S_{U,\rho} = \frac{\partial FOM_U / FOM_U}{\partial \rho / \rho} = -1.0, \tag{2.22}$$

$$S_{U,C_p} = \frac{\partial FOM_U / FOM_U}{\partial C_p / C_p} = -0.5 \tag{2.23}$$

$$S_{U,\mu} = \frac{\partial FOM_U / FOM_U}{\partial \mu / \mu} = 0.5 \tag{2.24}$$

The sensitivity of each property for the figure-of-merit of pumping power (FOMP) can be calculated by normalized form as follows:

$$S_{P,k} = \frac{\partial FOM_P / FOM_P}{\partial k / k} = -2.06, \tag{2.25}$$

$$S_{P,\rho} = \frac{\partial FOM_P / FOM_P}{\partial \rho / \rho} = -2.0, \tag{2.26}$$

$$S_{P,C_p} = \frac{\partial FOM_P / FOM_P}{\partial C_p / C_p} = -1.375, \tag{2.27}$$

$$S_{P,\mu} = \frac{\partial FOM_P / FOM_P}{\partial \mu / \mu} = 1.625. \tag{2.28}$$

According to the normalized form for the scaled pumping power, they have nearly identical value of sensitivity of thermal conductivity and density. That means the conductivity and density almost same effect on the pumping power.

The above scaling parameters can be widely accepted for comparisons of fluid thermal performance and optimization of channel geometries among various coolants. Finally, to compare and evaluate the performance of each coolant, ratio of the FOM can be defined as:

$$S_U = \frac{FOM_U}{FOM_{U,ref}}, \tag{2.29}$$

$$S_P = \frac{FOM_P}{FOM_{P,ref}}. \tag{2.30}$$

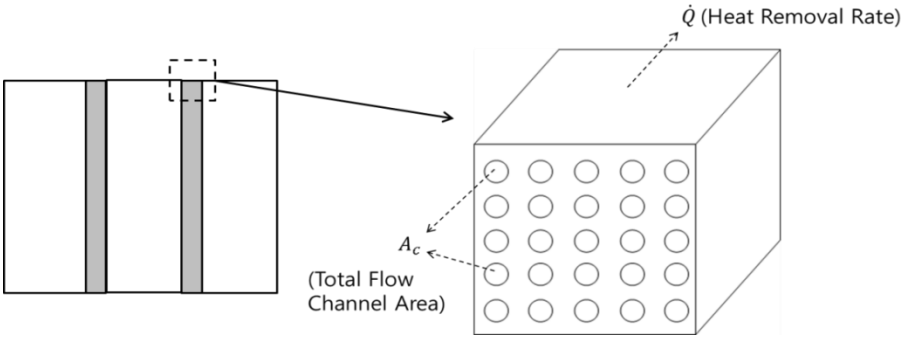

Figure 2.1 General Channel Structure in Solid Blanket

Chapter 3

Evaluation of Cooling Performance on Various Gas Mixtures

In this chapter, heat transfer capacity of each mixture gas is compared to each other by ratio of the FOM. This contains the method for evaluation and the mixture properties model for obtaining the properties of mixtures which are required for calculating the ratio of figure-of-merit. By following the evaluation methods, the heat transfer performance of binary gas mixtures and ternary gas mixtures is evaluated. Moreover, binary gas mixtures and ternary gas mixtures are compared.

As fusion blanket coolants, the helium is considered as a major candidate for gas coolant. Therefore, the evaluation is conducted on helium based gas mixtures. Carbon dioxide, xenon, krypton, neon, argon, nitrogen and steam are considered as mixed gas. In addition to this, evaluation on ternary gas mixtures is conducted with following three combinations of gas mixtures; helium-carbon dioxide-xenon mixtures, helium-carbon dioxide-krypton mixture and helium-krypton-xenon mixture.

3.1 Evaluation Method

The following steps of analysis show the procedure: how to estimate the scaling parameters which are proposed in previous chapter for optimization of the heat transport component.

Step 1: Thermal-hydraulic analysis using a computational fluid dynamics code or design code for a reference heat transport component design and coolants. In this step, the reference thermal conditions are obtained.

Step 2: Change of fluids and estimation of the new properties such as thermal conductivity, density, heat capacity, and viscosity. The properties are estimated using NIST database (National Institute of Standards and Technology database; Lemmon et al., 2007) based on presumed temperature, pressure, and compositions.

Step 3: Estimation of the new velocity and pumping power of the coolant and conditions using Eq. (2.29) and Eq. (2.30) which can achieve the same heat removal rate.

Step 4: Evaluation and optimization of the new fluid in terms of fluids conditions, such as pressure and compositions.

The calculations are conducted using EES (Engineering Equation Solver; Klein et al., 2007) program. The material properties of mixture gas are also calculated from the EES program based on mixture properties model.

The FOM of helium which has 700 K temperature and 8 MPa pressure is selected as the reference for the ratio of FOM. Therefore, temperature and pressure of helium in this condition has the 1.0 value of the ratio of FOM both for

velocity and pumping power.

Thus, the ratio of FOM of pumping power less than 1.0 implies the enhancement of heat transfer performance. This is because, the ratio of FOM less than 1.0 means that the comparing coolant is required lower pumping power than the reference case for achieving the same heat transfer performance. Furthermore, the ratio of FOM more than 1.0 indicates contrary circumstances of the previous case. Thus, the ratio of FOM can be applied for comparison of heat transfer performance for gas mixtures.

3.2 Mixture Property Model

The derived correlation is estimated by only properties of coolants. Thus, precise properties of mixture gas need to be calculated. For reaching this purpose, approach by Graham et al (1846) which is widely accepted for mixture gas is considered. In this approach, gas mixture properties have been determined by mole fraction weighted expressions. Therefore, the density of mixture gas is calculated as:

$$\rho_{mix} = \sum X_i \rho_i \,. \tag{3.1}$$

The conductivity of mixture gas is calculated as:

$$k_{mix} = \sum X_i k_i \,. \tag{3.2}$$

The heat capacity of mixture gas is calculated as:

$$C_{p,mix} = \sum X_i C_{p,i} \tag{3.3}$$

However, the viscosity estimated by mole fraction weighted expression is not allowable. (Davidson T. A., 1993) Because this model is suitable for mixtures of which components have nearly same molecular weight. However, that of helium and xenon are very different. Eventually, viscosity is calculated by another approach which is the equation of Herning and Zipperere (1936). Moreover, this approach has advantage of simple form: partial viscosities can be derived without the coefficients of Wilke (1950). Therefore the viscosity of mixture gas is calculated as:

$$\mu_{mix} = \frac{\sum X_i \mu_i (M_i)^{1/2}}{\sum X_i (M_i)^{1/2}} . \quad (3.4)$$

3.3 Evaluation on Cooling Performance for Binary Gas Mixtures

Heat transfer performance of helium and CO2 mixtures has been evaluated using scaled pumping power and velocity correlations. The evaluations for helium and carbon dioxide mixtures are carried out with the 8 MPa and 700 K conditions, and the results are illustrated in Fig. 3.1 and Fig. 3.2. The estimated pumping power of the carbon dioxide is higher than that of helium. However, the pumping power of gas mixtures showed a nonlinear relation between the pumping power of pure helium and carbon dioxide. Moreover, the pumping power of mixture gas is estimated lower than that of pure helium and pure carbon dioxide.

The ratio of FOMp has the minimum point at the 0.4 mole fraction of carbon

dioxide. Furthermore, curve of the scaled pumping power is flat around optimal points. Then, it can be deduced that mixture gas which has minimum pumping power is the stable condition for the pumping powers with changing the mole fraction of the component gas.

The ratio of FOM with helium and carbon dioxide mixture has been evaluated with the various temperature and pressure and the results are indicated in the Fig. 3.3 and Fig. 3.4. The relative minimum scaled pumping power which is a ratio of pumping power of each case are calculated and listed in Table 3.1 and 3.2. The results demonstrate that cooling performance of gas mixtures are enhanced in case of low pressure and low temperature. Mixture gas in condition of operating pressure 4 MPa has better heat transfer capacity compared to pure helium gas of operating pressure 8 MPa. Generally the low operating pressure is beneficial in aspect of leakage and safety. This means that the mixture gas has both of better cooling capability and safety.

Pumping powers of helium and other gas mixture have been evaluated as illustrated in Fig. 3.5. Other mixed gases have been taken into account argon, neon, krypton, xenon, nitrogen and steam. The results shows that the minimum points of scaled pumping power are located around 0.4 of the mole fraction of additive gas. The mixed gas which has a relatively high density such as xenon and krypton has a good performance of heat transfer as shown in Fig. 3.6 and Table 3.3. The results show that by using xenon as a mixed gas, only 4% of pumping power is needed comparing with pure helium coolant. Moreover, only 26% of that is required in case of using the argon which is easy to find as a mixed gas.

The mechanism for enhancement of heat transfer can be explained using the sensitivity of each property for the FOM. The sensitivity of each property for the

FOM is listed in the Table. 3.4. Helium gas has high thermal conductivity but has very low density. Mixture with heavy fluid with moderate thermal conductivity can compensate a negative impact on heat transfer performance by low density. In particular, sensitivity of fluid density and the thermal conductivity have close value. This means that the effects of density and thermal conductivity on cooling performance are almost same. However, thermal conductivity of mixture gas is six times larger than that of pure helium. Moreover, density of mixture gas is half of that of pure helium as illustrated in Table. 3.5. Because the density and thermal conductivity have almost same effect on cooling performance, that of gas mixture can be enhanced.

3.4 Evaluation on Cooling Performance for Ternary Gas Mixtures

Heat transfer performance of ternary gas mixtures are evaluated in terms of the scaled pumping power. Carbon dioxide, krypton and xenon are taken into account as the combined gases, which have high heat transfer performance as a mixed gas for binary mixture. Over than 5000 data are estimated for ternary gas mixtures by increasing mole fraction 0.01. The minimum scaled pumping power, and the mole fraction of component gases are listed in Table 3.6. And the log scaled pumping power of ternary gas mixtures are plotted in Fig. 3.7 – 3.12.

3.5 Comparison of Binary and Ternary Gas Mixtures

Optimum point for scaled pumping power doesn't exist at three component gas mixture region. It was concluded that there are no benefits on cooling capability. This is resulted from the pumping powers of binary gas mixtures and the properties of that. Minimum points of scaled pumping powers are located between 0.3 and 0.5 mole fraction of additive gas. And the curves of the scaled pumping power don't have the point of intersection as shown in Fig. 3.13. This tendency of scaled pumping power make the lowest point of scaled pumping power doesn't exist in the ternary gas mixture region.

Moreover the lines of material properties don't have the intersecting point except the viscosity as illustrated in Fig. 3.14 – 3.17. These results came from the properties mixtures model based on mole fraction weighted expression. Therefore, the lines of properties except the viscosity have linear characteristic which are determined by the properties of pure component gas. Finally, the optimal points of the scaled pumping power which are determined by properties of gas mixture cannot exist on the ternary gas mixture region.

Table 3.1 Scaled pumping power of helium and carbon dioxide mixture with pressure

Pressure [MPa]	Relative minimum S_P
2	0.0682
4	0.0709
6	0.0709
8	0.0725
10	0.0741
12	0.0758

Table 3.2 Scaled pumping power of helium and carbon dioxide mixture with temperature

Temperature[K]	Relative minimum S_P
500	0.058
700	0.072
900	0.086
1100	0.098

Table 3.3 Minimum scaled pumping power of other gas mixtures

Mixed gas	Relative minimum S_P
Xenon	0.041
Krypton	0.094
CO_2	0.131
Argon	0.262
Steam	0.305
Nitrogen	0.313
Neon	0.708

Table 3.4 Sensitivity of properties of gas mixtures

Parameter	Sensitivity of properties
Fluid Density	$S_{P,k} = \frac{\partial FOM_P / FOM_P}{\partial k / k} = -2.06$
Thermal Conductivity	$S_{P,\rho} = \frac{\partial FOM_P / FOM_P}{\partial \rho / \rho} = -2.0$
Heat Capacity	$S_{P,C_p} = \frac{\partial FOM_P / FOM_P}{\partial C_p / C_p} = -1.375$
Viscosity	$S_{P,\mu} = \frac{\partial FOM_P / FOM_P}{\partial \mu / \mu} = 1.625$

Table 3.5 Mechanism for enhancement of heat transfer performance

	He	→	0.5He + 0.5CO_2	CO_2
Thermal conductivity	5.4 (~0)	×6 →	30	60.4
Density	0.28	×1/2 →	0.14	0.05 (~0)

Table 3.6 Scaled pumping power of ternary mixture gas

Case	Mole fraction of component gas			Scaled pumping power
He-CO_2-Xe	He	CO_2	Xe	4.00E-02
	0.65	0	0.35	
He-CO_2-Kr	He	CO_2	Kr	9.33E-02
	0.67	0	0.33	
He-Kr-Xe	He	Kr	Xe	4.00E-02
	0.65	0	0.35	

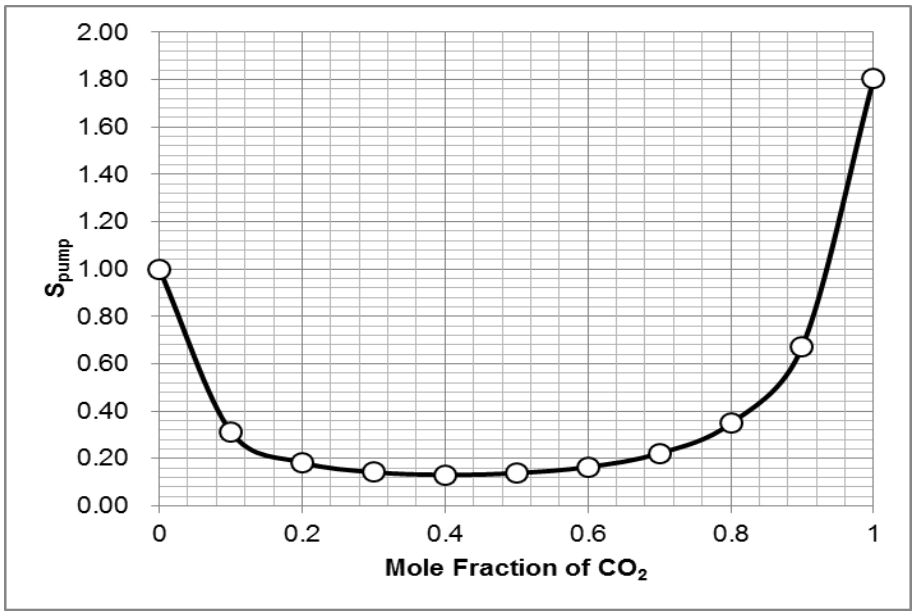

Figure 3.1 scaled pumping power of helium and carbon dioxide mixture

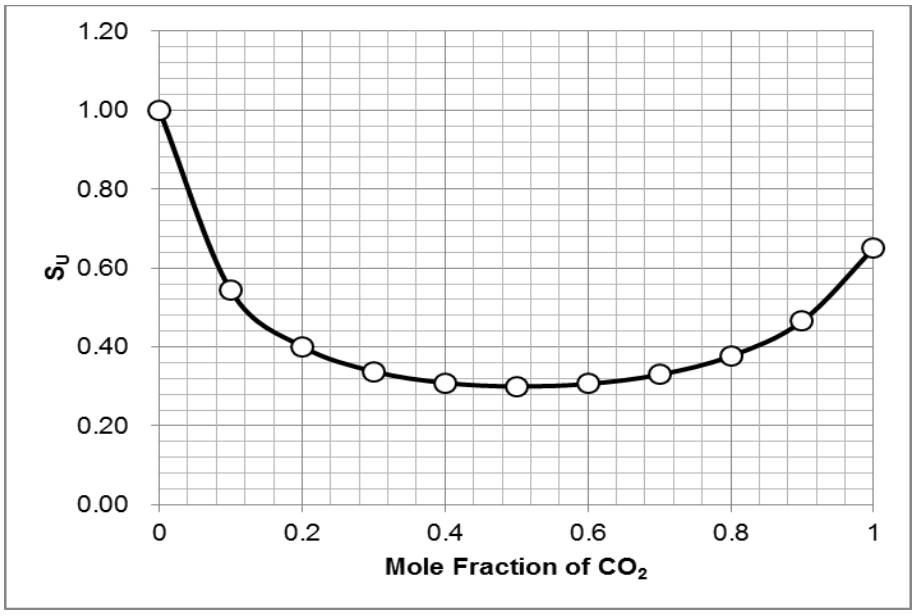

Figure 3.2 scaled velocity of helium and carbon dioxide mixture

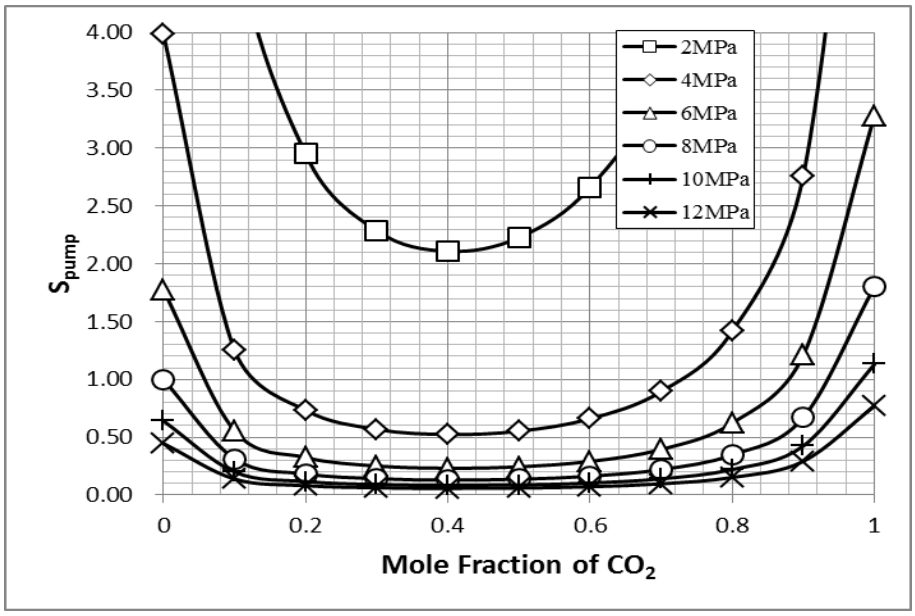

Figure 3.3 scaled pumping power of helium and carbon dioxide mixture with pressure

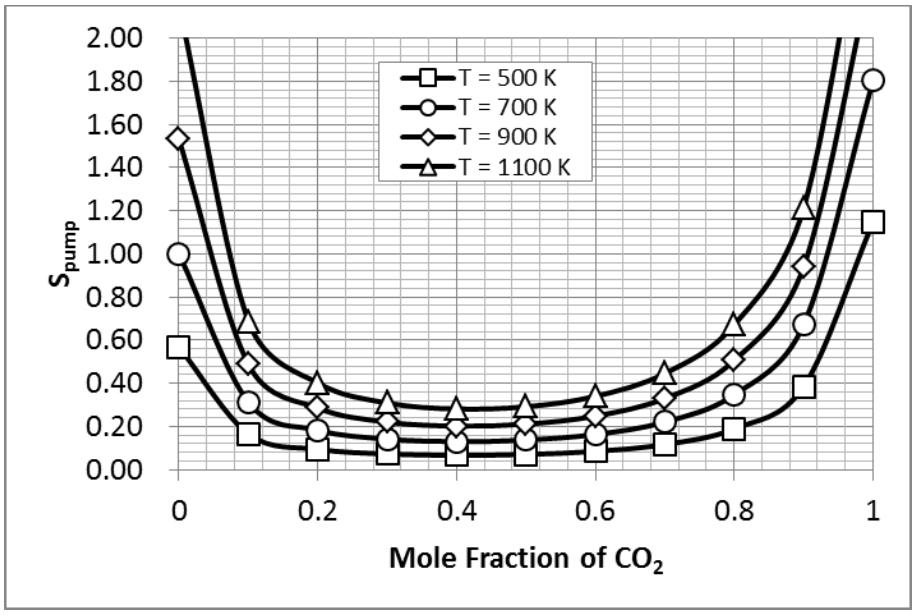

Figure 3.4 scaled pumping power of helium and carbon dioxide mixture with temperature

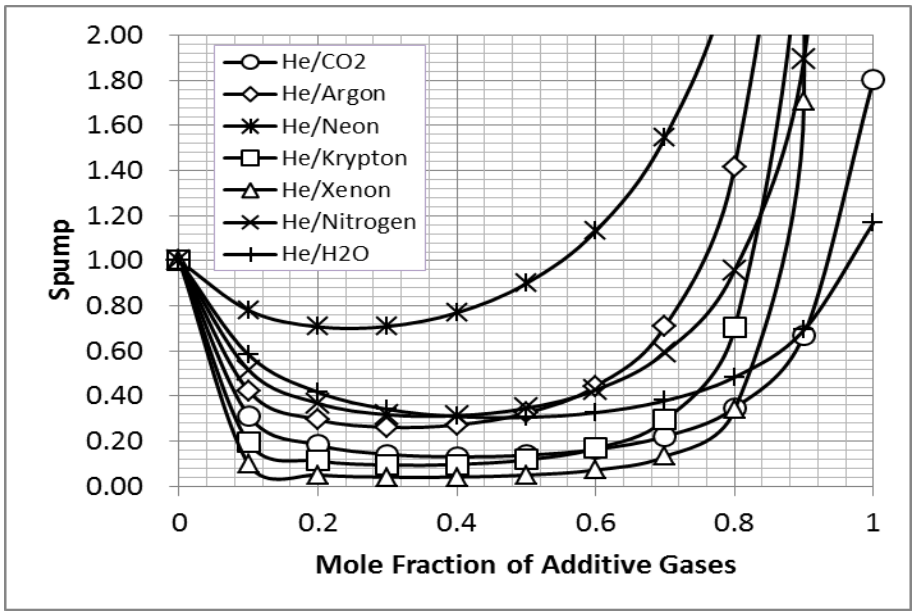

Figure 3.5 scaled pumping power of gas mixtures

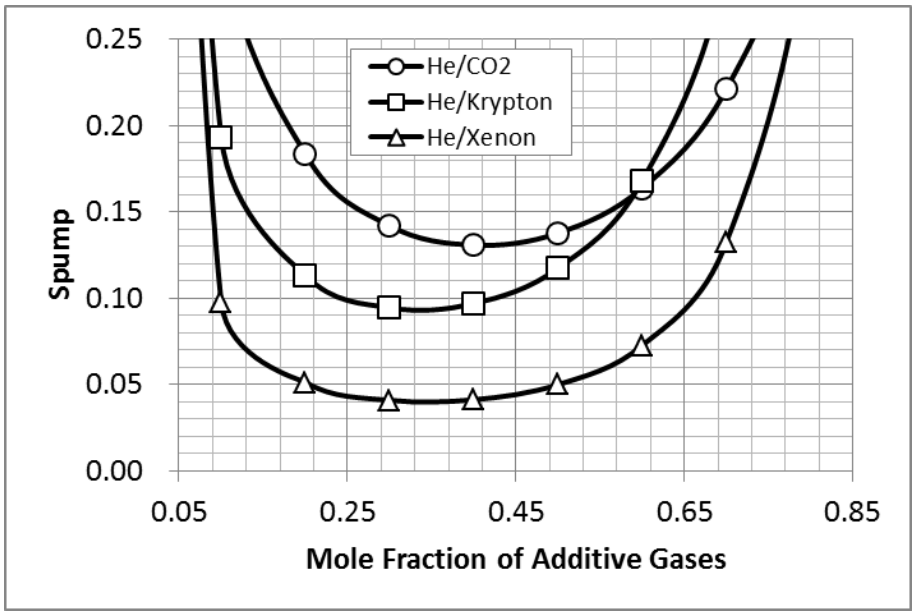

Figure 3.6 scaled pumping power of helium with carbon dioxide, krypton and xenon mixtures

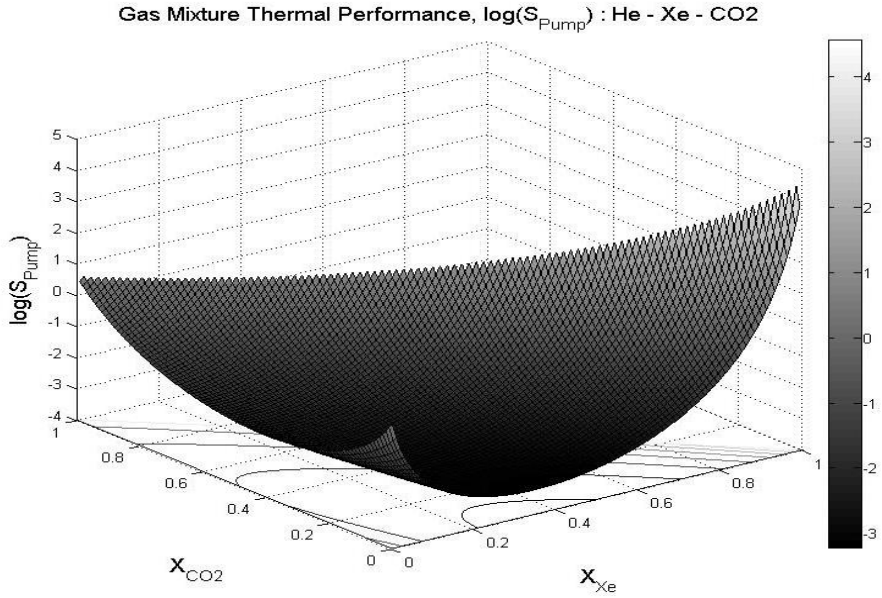

Figure 3.7 Scaled pumping power of helium, xenon and carbon dioxide mixture (3D plot)

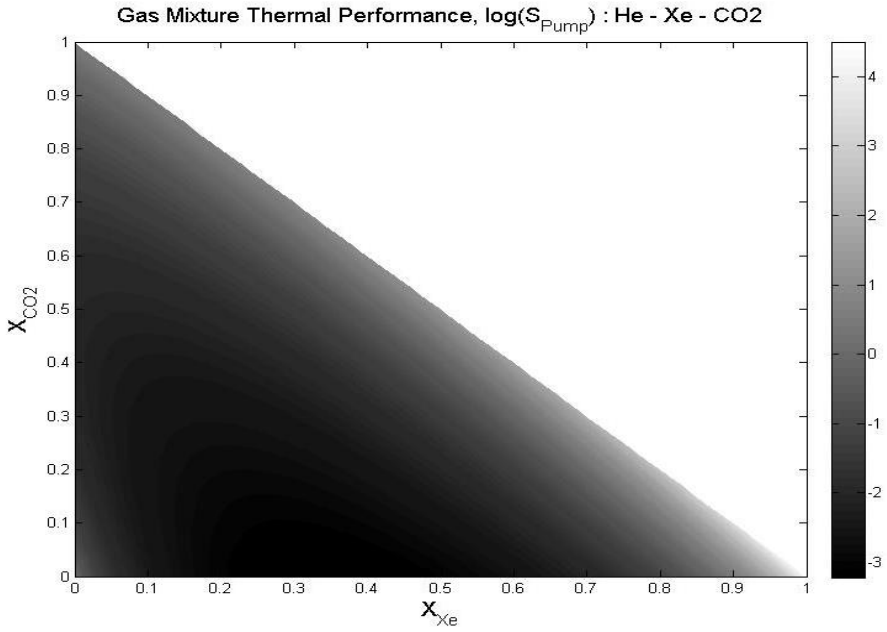

Figure 3.8 Scaled pumping power of helium, xenon and carbon dioxide mixture (contour)

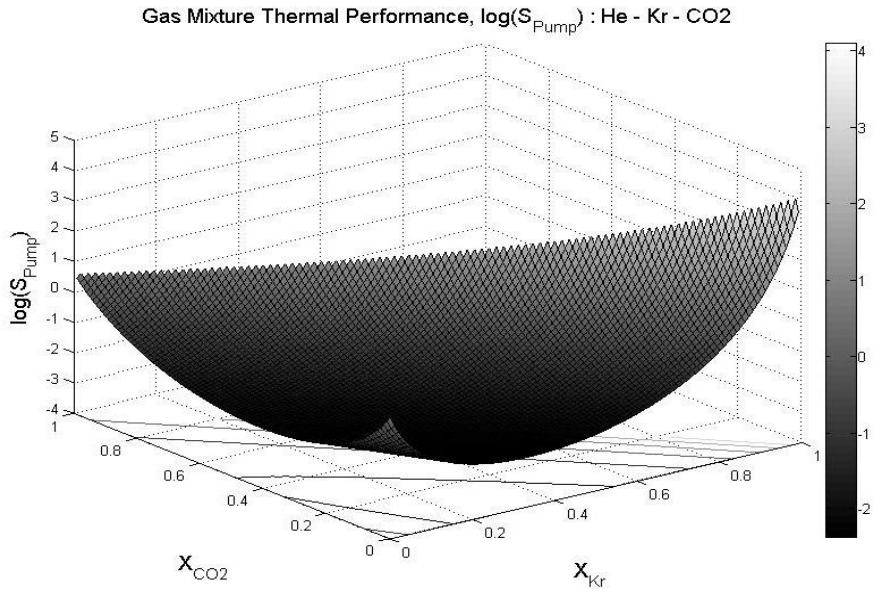

Figure 3.9 Scaled pumping power of helium, krypton and carbon dioxide mixture (3D plot)

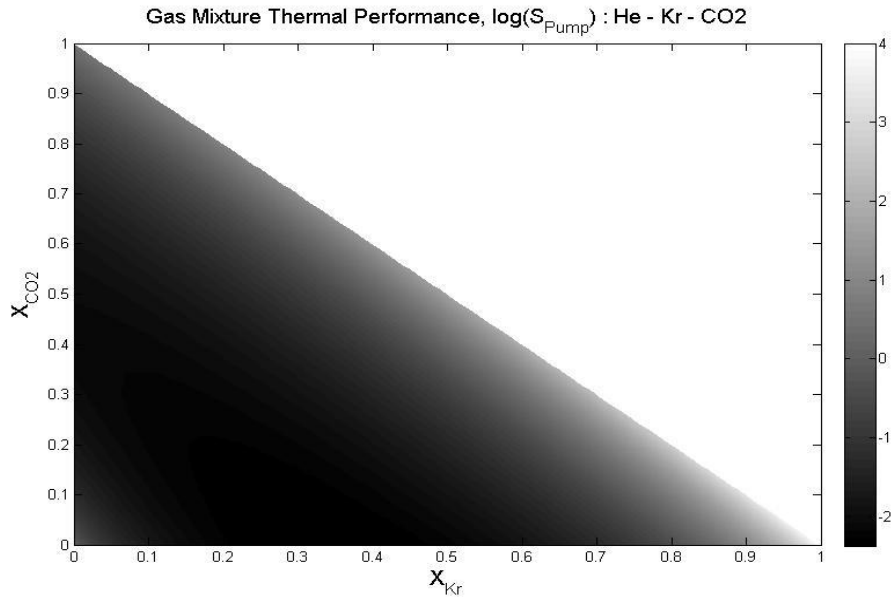

Figure 3.10 Scaled pumping power of helium, kryptonand carbon dioxide mixture (contour)

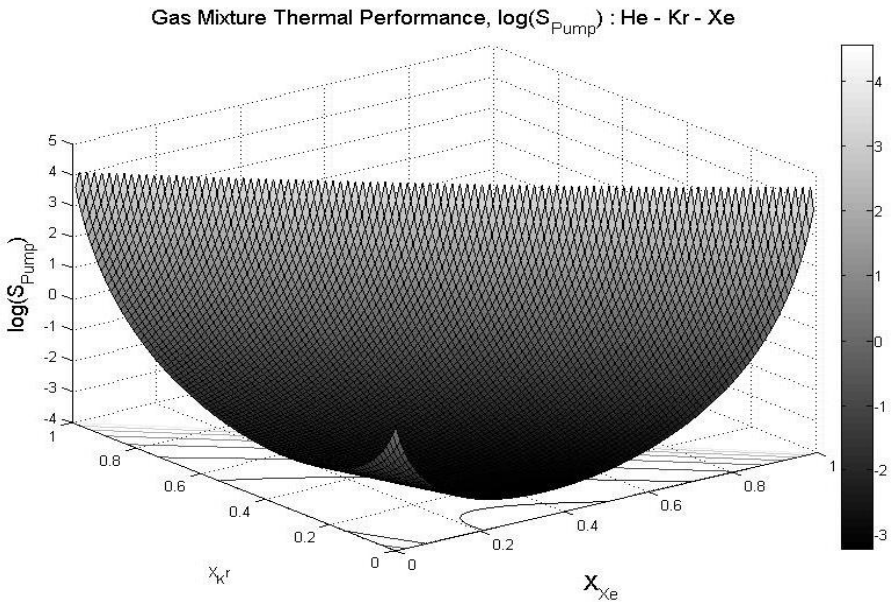

Figure 3.11 Scaled pumping power of helium, xenon and krypton (3D plot)

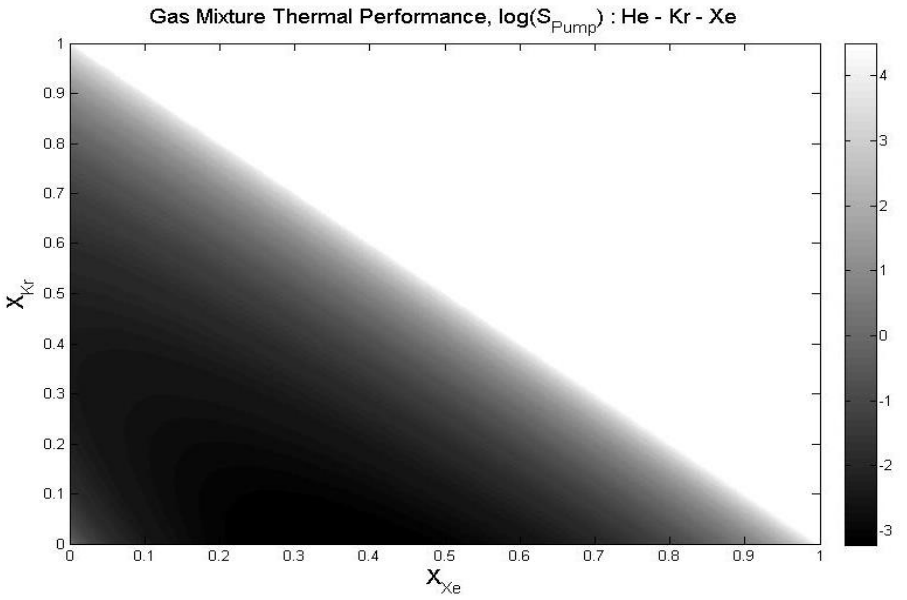

Figure 3.12 Scaled pumping power of helium, xenon and krypton (contour)

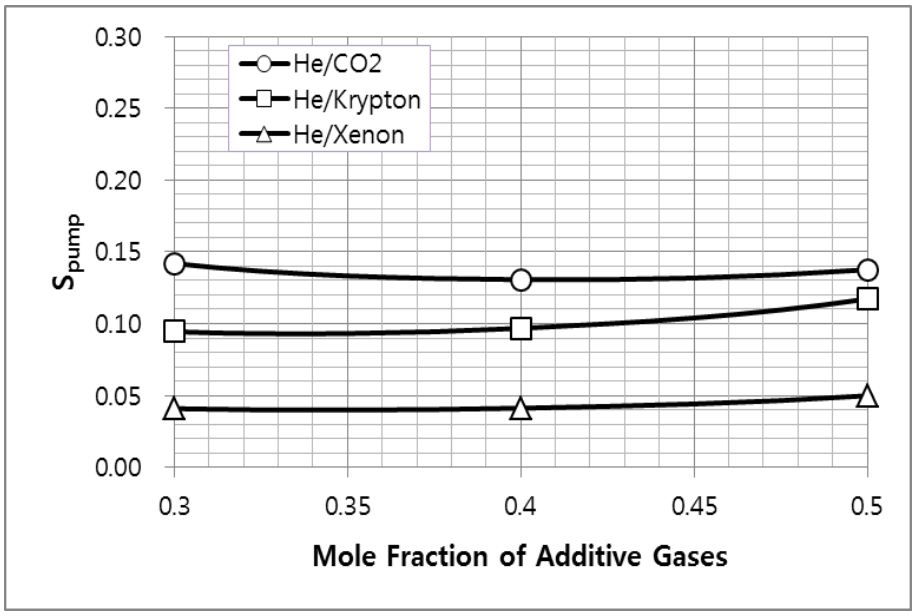

Figure 3.13 Scaled pumping power around optimal point

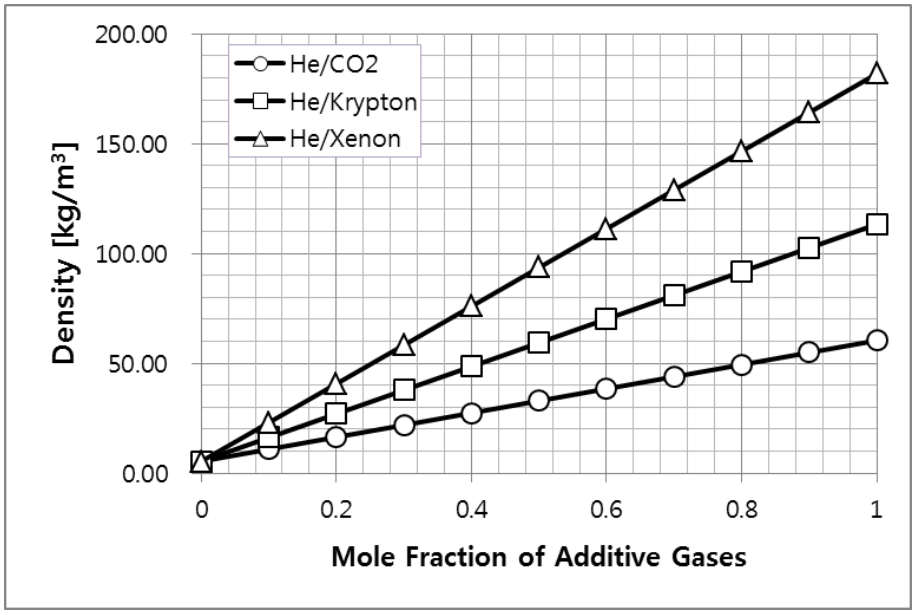

Figure 3.14 Density of gas mixture

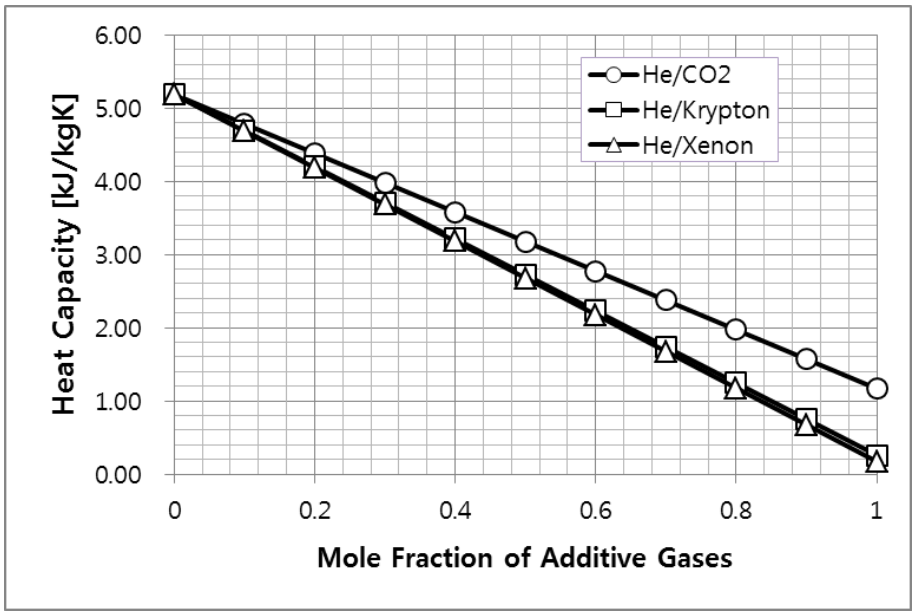

Figure 3.15 Heat capacity of gas mixture

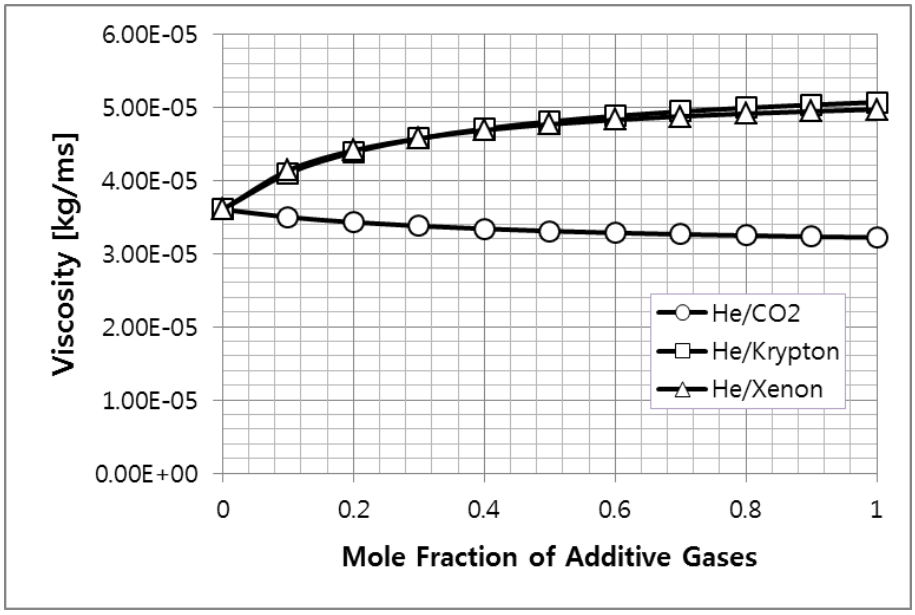

Figure 3.16 Viscosity of gas mixture

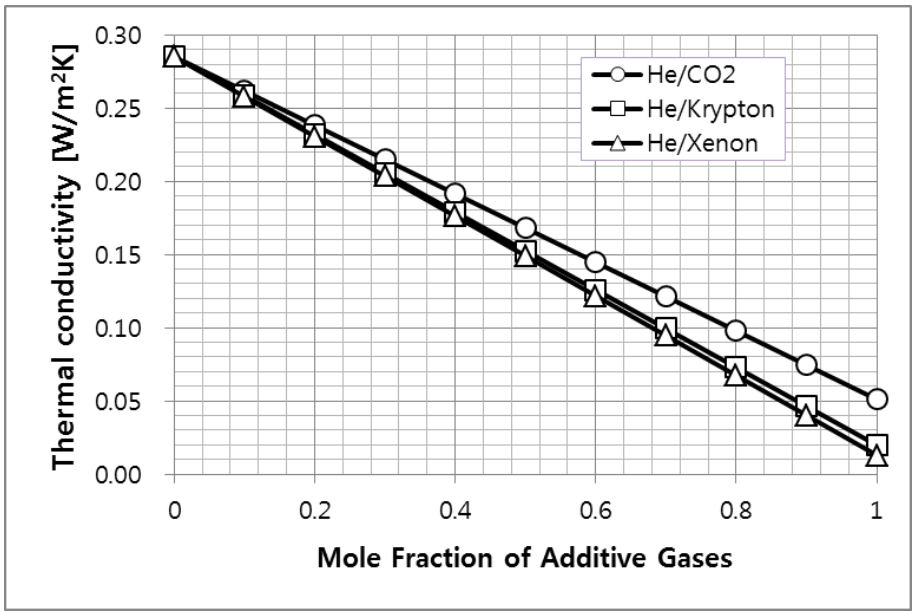

Figure 3.17 Thermal conductivity of gas mixture

Chapter 4

Validation of Thermal Performance Enhancement using CFD Simulation

In this chapter, the validation for developed correlation is conducted. This contains the description of validation model including geometry and boundary condition of that. Moreover, in aspect of CFD (Computational Fluid Dynamics) analysis, grid model and physics model are included. The method for validation is described in detail and the results are illustrated in this chapter.

Validation is focusing on the velocity and pumping power. The velocity which makes same temperature distribution of validation model is carried out with changing that. This is because same temperature distribution can represent the same heat transfer performance and it is suitable for constraints of developed correlation. And also, the pumping power is derived each cases. Moreover, the velocity and pumping power is compared with that of reference case. Those have identical signification with ratio of FOM. Thus, the developed correlation can be validated with CFD simulation.

The calculation results of the developed correlations have a good agreement with validation results. However, there is small discrepancy between correlation and validation results. Thus, sensitivity tests including heat transfer coefficient

and frictional form loss are conducted. Moreover, the error of derived correlation due to that of heat transfer coefficient is determined.

4.1 Case and Model Description: ITER HCML TBM

The Korean Helium Cooled Molten Lithium (HCML) Test Blanket Module (TBM) is designed by KAERI (Lee et al., 2007) to be tested in International Thermonuclear Experimental Reactor (ITER). The HCML TBM is designed using helium as a coolant and molten lithium as a tritium breeder. The schematic view and cross-sectional view are illustrated in Fig. 4.1 and Fig. 4.2.

Reduced Activation Ferrite Martensitic (RAFM) steel is selected for the structural material. The maximum temperatures are restricted as 550 ℃. (Zinkle and Ghoniem, 2000) In aspect of same heat transfer performance which is constraint for the developed correlation, that is restricted by temperature window. This means that the validation is performed with practical condition of nuclear fusion blanket. Moreover, HCML TBM is suitable model to validate developed correlation. The reason is that HCML TBM has appropriate geometry for developed correlation which is described in previous chapter.

Thermal hydraulic characteristics of HCML TBM have been carried out using CFD analysis under helium coolant condition. (Lee et al., 2006) The validation is conducted based on previous analysis. The gas mixture which is compounded with helium and carbon dioxide is selected for validation. The coolant is different with that of previous study. The validation cases are listed at Table. 4.1.

4.2 Geometry and Grid Model

HCML TBM can be divided into a first wall region and breeding zone region. The first wall region has a purpose to remove the surface heat from the plasma, and breeding zone is aimed to breed the tritium in the suitable temperature of multiplier and breeder. (Enoeda et al., 2003) Thus, the characteristics of heat transfer including temperature distribution are important for both first wall region and breeding zone.

The first wall region of HCML TBM has 60 coolant channels, and the breeding zone has 35 coolant channels. The cooling channels of the breeding zone have straight duct geometry. However, those of first wall have curved shape. The size of coolant channels in of both first wall and breeding zone is identical between them as illustrated in Fig. 4.3 and 4.4.

Validation model has 3,580,999 of hexahedra meshes and the number of elements for each part as listed in Table. 4.2. The meshes are separately created for fluid and structure which is including lithium and graphite and grid, after that the meshes are combined for analysis as illustrated in Fig. 4.7. The mesh grid of first wall channel is illustrated in Fig. 4.6. The full height of breeding zone consists of structure, lithium, graphite, and helium flow. Among them, manifold and covers are not included. (Lee et al., 2006)

4.3 Physical Model

CFX-13 which is widely used as one of the CFD codes is based on Finite Volume Method (FVM) for partial differential equations. In this study, the steady-state solution is computed. Reynolds Averaged compressible Navier-Stokes (RANS) model is adopted as a solver with the standard k-ε turbulence model. This model is commonly accepted to analyze heat transfer between solid and turbulent gas. Moreover, HCML TBM is estimated by same model in previous study. (Lee et al., 2007) Governing equation for continuity and momentum can be expressed as:

$$\frac{\partial \rho}{\partial t} + \frac{\partial}{\partial x_j}\left(\rho U_j\right) = 0\,, \tag{4.1}$$

$$\frac{\partial \rho U_i}{\partial t} + \frac{\partial}{\partial x_j}\left(\rho U_i U_j\right) = -\frac{\partial p'}{\partial x_i} + \frac{\partial}{\partial x_j}\left(\mu_{eff}\left(\frac{\partial U_i}{\partial x_j} + \frac{\partial U_j}{\partial x_i}\right)\right) + S_M\,, \tag{4.2}$$

where S_M is some of the body forces, p' represents the modified pressure and can be expressed as:

$$p' = p + \frac{2}{3}\rho k + \frac{2}{3}\mu_{eff}\frac{\partial U_k}{\partial x_k}\,. \tag{4.3}$$

μ_{eff} represents the effective viscosity for turbulence as:

$$\mu_{eff} = \mu + \mu_t\,, \tag{4.4}$$

where μ_t is turbulence viscosity :

$$\mu_t = C_\mu \rho \frac{k^2}{\varepsilon}\,, \tag{4.5}$$

where C_μ is denotes *k-ε* turbulence model constant.

And the *k*-ε turbulence model can be written as;

$$\frac{\partial(\rho k)}{\partial t}+\frac{\partial}{\partial x_j}(\rho U_j k)=\frac{\partial}{\partial x_j}\left[\left(\mu+\frac{\mu_{\mathrm{T}}}{\sigma_{\mathrm{k}}}\right)\frac{\partial k}{\partial x_j}\right]+P_{\mathrm{k}}-\rho\varepsilon+P_{\mathrm{kb}}, \tag{4.6}$$

$$\frac{\partial(\rho \varepsilon)}{\partial t}+\frac{\partial}{\partial x_j}(\rho U_j \varepsilon)=\frac{\partial}{\partial x_j}\left[\left(\mu+\frac{\mu_{\mathrm{T}}}{\sigma_{\varepsilon}}\right)\frac{\partial \varepsilon}{\partial x_j}\right]+\frac{\varepsilon}{k}(C_{\varepsilon 1}P_{\mathrm{k}}-C_{\varepsilon 2}\rho\varepsilon+C_{\varepsilon 1}P_{\varepsilon b}), \tag{4.7}$$

where μ_{T} is turbulent viscosity, P_{kb} and $P_{\varepsilon b}$ denote the influence of the buoyancy forces. P_{k} represents the turbulence production because of viscous forces. $C_{\varepsilon 1}$, $C_{\varepsilon 2}$ and σ_{ε} denote *k*-ε turbulence model constant.

The turbulence production due to viscous forces is as following.

$$P_{\mathrm{k}}=\mu_{\mathrm{T}}\left(\frac{\partial U_i}{\partial x_j}+\frac{\partial U_j}{\partial x_i}\right)\frac{\partial U_i}{\partial x_j}-\frac{2}{3}\frac{\partial U_k}{\partial x_k}(3\mu_t\frac{\partial U_k}{\partial x_k}+\rho k). \tag{4.8}$$

And heat transfer equation can be described as:

$$\frac{\partial(\rho h)}{\partial t}+\nabla\cdot(\rho U_s h)=\nabla\cdot(\lambda\nabla T)+S_E, \tag{4.9}$$

where h and λ are enthalpy and thermal conductivity of solid. S_E denotes an optional volumetric heat source. U_s represent the solid velocity.

4.4 Boundary Condition

Due to the temperature window of the structural material, HCML TBM was designed not to exceed 550 ℃ for the maximum temperature of the structural material. Satisfying this design window, the major design parameter of HCML TBM is deducted in the previous study (Lee et al., 2007). And the major design parameters are listed in Table. 4.3.

The cooling system of HCML TBM is illustrated in Fig. 4.8. Helium flow is cooling the first wall foremost with 1.22 kg/sec of mass flow and 50 m/s of velocity. And then, the helium flows are divided half, each flow goes into the top and bottom cover with 0.61 kg/sec of mass flow. Helium flow has upward flow with 26.316 m/sec of velocity in the front region. Another helium flow has downward flow with 31.250 m/sec of velocity in rear region. After cooling the breeding zone two helium flows are combined, and it is released through the back wall.

The helium temperature is rising with cooling the first wall and breeding zone. That of helium is also calculated in the previous study for HCML TBM. (Lee et al., 2007) This is applied to determine the initial condition of fluid inlet temperature. The results of the temperature are illustrated as Fig. 4.9. Thus, inlet temperature of first wall cooling channel organized into three parts and each part has 300 ℃, 320 ℃ and 340 ℃ of temperature. And also, that of breeding zone cooling channel has 360 ℃. These helium temperatures are accepted as inlet temperature of the validation present in the same manner of the previous study.

The heat source of HCML TBM consists of surface heat from plasma and neutron heat source. The surface heat source has 0.3 MW/m2 in average condition

and 0.5 MW/m2 at peak condition as listed Table 4.3. The neutron heat source which is the other heat source of HCML TBM is calculated in the previous study. (Lee et al., 2007) The power density of each region is calculated according to the distance from plasma side as illustrated in Fig. 4.10.

4.5 Validation Method

Various steady Coolant channels in HCML TBM are composed of first wall channel and grid channel. Those are classified as described in below for estimating the fluid characteristic such as pressure distribution and mass flow rate. First wall channels consist of Fist wall top channels, Fist wall middle channels and First wall bottom channels. In addition for convenience, grid channels are categorized as Grid 01 left channels, Grid 01 middle channels, Grid 01 right channels, Grid 02 left channels, Grid 02 right channels, Grid 03 left channels, and Grid 03 right channels, as illustrated in Fig 4.11 and 4.12.

Mass flow rate and pressure drop of each classified channel are calculated in CFD code. Pumping powers of the validation cases are derived by mass flow rate and pressure drop. Process of calculating pumping powers is following these steps:

Step 1: Mass flow rate data in an inlet boundary of all channels are exported from the CFD codes.

Step 2: Pressure drop data on the grid line and first wall line are exported from the CFD codes.

Step 3: Volumetric flow rate is calculated using mass flow rate and density of

gas mixtures.

Step 4: Pumping power is calculated using volumetric flow rate and pressure drop data. There is assumption that pump efficiency is identical in every case.

The volumetric flow rate and the pumping power are expressed as:

$$G = \dot{m} / \rho, \tag{4.10}$$

$$P_P = \frac{G \cdot \Delta p}{\eta}. \tag{4.11}$$

The ratio of the pumping power which is normalized by reference pumping power is determined in the CFD calculation. This has same physical meaning with the ratio of the pumping power in developed correlation. Thus, validation is conducted using the ratio of the pumping powers of CFD calculation and developed correlation. The ratio of pumping power is calculated as:

$$S_{P,CFD} = \frac{P_{P,mix}}{P_{P,ref}}. \tag{4.12}$$

Velocity which is one of the boundary conditions of HCML TBM analysis is changed for validation. The maximum temperatures of line 1 to 6 are used as a variable for validation data. Those in order to obtain the temperature distribution are illustrated in Fig. 4.11 and 4.12. The validation is conducted until the RMS (Root Mean Square) errors of temperature difference become around 1.0 in each case.

4.6 Calculation Results

The results of maximum temperature on the lines and ratio of pumping powers using CFD are expressed in Table 4.4. Validation results and RMS errors in temperature difference are presented in Table 4.5 and Table 4.6. The ratio of scaled velocity and that of scaled pumping power are described in Fig. 4.12 and Fig. 4.13 for validation. The results show that validation data which is determined from CFD has good agreement with the derived correlation in terms of achieving the same heat transfer performance. However, the difference increases with high mole fraction of carbon dioxide. To find a reason for this discrepancy, Reynolds number and Prandtl number of fluid conditions of mixture gases are checked as described in Fig. 4.14. The box with a slash-pattern is signifying the valid range of the Dittus-boelter correlation. The Dittus-boelter correlation can be used when,

$$10^4 \le \mathrm{Re} \le 1.24 \times 10^5, \tag{4.13}$$

$$0.7 \le \mathrm{Pr} \le 120. \tag{4.14}$$

In the case of the helium and carbon dioxide gas mixture, the Prandtl number is not perfectly suitable for valid range of the Dittus-boelter correlation. As the mole fraction of carbon dioxide increases, the Reynolds numbers increases distinctively. The Reynolds number is passing through and become ten times as the maximum for the Dittus-boelter correlation. Thus, Kays and Crawfold correlation is tested for sensitivity of correlation. This is because, that is heat transfer correlation satisfying the Reynolds and Pradtl number for validation case. The Kays and Crawfold correlation can be used when,

$$10^4 \le \mathrm{Re} \le 5 \times 10^6, \tag{4.15}$$

$$0.5 \le \mathrm{Pr} \le 1. \tag{4.16}$$

This correlation has the suitable range for Reynols number and Prandtl number as shown in Fig. 4. 15.

The Kays and Crawfold correlation has the same form of equation with the Dittus-Boelter correlation. Thus, the scaled parameter using the Kays and Crawfold correlation can be derived with a similar procedure which is derivation of FOM using the Dittus-Boelter correlation.

Heat transfer coefficient was calculated by Kays and Crawfold correlation as follows.

$$h = \frac{k}{D_e} \cdot Nu = \frac{k}{D_e} \cdot \left(0.022\,\mathrm{Re}^{0.8}\,\mathrm{Pr}^{0.5}\right). \tag{4.17}$$

By combining equation (4.17), (2.2) and (2.3) the heat transfer coefficient can be expressed by:

$$h = 0.023 \cdot (k)^{0.5} (\rho)^{0.8} (C_p)^{0.5} (\mu)^{-0.5} (D_e)^{-0.2} (U)^{0.8}. \tag{4.18}$$

Therefore, the flow velocity can be written by:

$$U = (118.02) \cdot (h)^{1.25} (k)^{-0.625} (\rho)^{-1} (C_p)^{-0.625} (\mu)^{0.625} (D_e)^{0.25}. \tag{4.19}$$

And using the same constraint written in equation (2.6) – (2.10), the velocity without the heat transfer coefficient term can be obtained as;

$$U = (118.02) \cdot \left(C_1 \left(\frac{D_e}{4 \cdot \alpha \cdot V} \right) \right)^{1.25} (k)^{-0.625} (\rho)^{-1} (C_p)^{-0.625} (\mu)^{0.625} (D_e)^{0.25}, \tag{4.20}$$

$$U \sim (k)^{-0.625} (\rho)^{-1} (C_p)^{-0.625} (\mu)^{0.625} (D_e)^{1.5} (\alpha)^{-1.25}. \tag{4.21}$$

Therefore, based on the Eq.(4.21), figure-of-merits for velocity to achieve the same heat transfer performance can be defined as follows.

$$FOM_{U,Kays} = \left(\frac{k}{k_0}\right)^{-0.625} \left(\frac{\rho}{\rho_0}\right)^{-1} \left(\frac{C_p}{C_{p0}}\right)^{-0.625} \left(\frac{\mu}{\mu_0}\right)^{0.625} \left(\frac{D_e}{D_{e0}}\right)^{1.5} \left(\frac{\alpha}{\alpha_0}\right)^{-1.25}. \tag{4.22}$$

That for the pumping powers can be derived by inserting Eqs. (4.20), (2.16), and (2.17) in Eq. (2.15), the following expression can be obtained as:

$$P_{pump} \sim \left\{ (k)^{-1.72} (\rho)^{-2.0} (C_p)^{-1.72} (\mu)^{1.97} \right\} \cdot \left\{ (D_e)^{2.875} (\alpha)^{-2.44} \right\}. \quad (4.23)$$

Thus, based on the Eq.(4.20), the figure-of-merits for pumping power can be derived as;

$$FOM_{P,Kays} = \left\{ \left(\frac{k}{k_0} \right)^{-1.72} \left(\frac{\rho}{\rho_0} \right)^{-2.0} \left(\frac{C_p}{C_{p0}} \right)^{-1.72} \left(\frac{\mu}{\mu_0} \right)^{1.97} \right\} \cdot \left\{ \left(\frac{D_e}{D_{e0}} \right)^{2.875} \left(\frac{\alpha}{\alpha_0} \right)^{-2.44} \right\}. \quad (4.24)$$

The scaled velocity and scaled pumping power using Kays Crawfold correlation are compared with validation data as illustrated in Fig. 4.16 and 4.17. The results showed that the valid range of Reynolds and Prandtl number has no significant effect on the difference of scaled velocity and pumping power in the high mole fraction of carbon dioxide.

The derived correlation doesn't consider the form loss pressure drop. So it is figured out that difference with scaled pumping power ratio calculated using correlation and validation data calculated using CFD come from form loss pressure drop. Thus, the scaled pumping power which is considering form loss is derived. The pressure drop considering the form loss is described as:

$$\Delta p = (f \cdot \frac{1}{2} \cdot \frac{L}{D_e} + K) \cdot \rho \cdot U^2 . \quad (4.25)$$

The length over hydraulic diameter is used as 100. This is because validation model has around 100 of that. Using the Blasius formula as described in the Eq. (2.16) the pressure drop considering form loss is derived as:

$$\Delta p = (\mathrm{Re}^{-0.25} \cdot \frac{1}{2} \cdot 50 + K) \cdot \rho \cdot U^2 . \quad (4.26)$$

To figure out the effect of form loss, the values which are 0.3 and 3 are used

described as:

$$\Delta p = (\mathrm{Re}^{-0.25} \cdot \frac{1}{2} \cdot 50 + 0.3) \cdot \rho \cdot U^2 , \tag{4.27}$$

$$\Delta p = (\mathrm{Re}^{-0.25} \cdot \frac{1}{2} \cdot 50 + 3) \cdot \rho \cdot U^2 . \tag{4.28}$$

For deriving the scaled pumping power, pressure drop need to be form of multiplication without addition. So, the form of pressure drop is changed by fitting the graph of pressure drop described as:

$$\Delta p = (11.5 \cdot \mathrm{Re}^{-0.25}) \cdot \rho \cdot U^2 , \tag{4.29}$$

$$\Delta p = (8.47 \cdot \mathrm{Re}^{-0.25}) \cdot \rho \cdot U^2 . \tag{4.30}$$

The scaled pumping power can be determined by pressure drop which is considering the frictional form loss. The method for deriving scaled pumping power considering form loss is same with the process of described equation in (2.14)-(2.19). Finally, the scaled pumping power can be expressed as

$$FOM_{P,K=0.3} = \left\{ \left(\frac{k}{k_0} \right)^{-2.1} \left(\frac{\rho}{\rho_0} \right)^{-2.0} \left(\frac{C_p}{C_{p0}} \right)^{-1.4} \left(\frac{\mu}{\mu_0} \right)^{1.6} \right\} \cdot \left\{ \left(\frac{D_e}{D_{e0}} \right)^{2.95} \left(\frac{\alpha}{\alpha_0} \right)^{-2.5} \right\}, \tag{4.31}$$

$$FOM_{P,K=3} = \left\{ \left(\frac{k}{k_0} \right)^{-2.2} \left(\frac{\rho}{\rho_0} \right)^{-2.0} \left(\frac{C_p}{C_{p0}} \right)^{-1.47} \left(\frac{\mu}{\mu_0} \right)^{1.54} \right\} \cdot \left\{ \left(\frac{D_e}{D_{e0}} \right)^{3.15} \left(\frac{\alpha}{\alpha_0} \right)^{-2.66} \right\}. \tag{4.32}$$

The scaled pumping power including frictional form loss is compared with validation data, and the original scaled pumping power as figured in Fig. 4.20. The results showed that the form loss is not related with the difference of the ratio of scaled pumping power, there is large discrepancy with the form loss.

To figure out the error of scaled pumping power due to that of the heat transfer coefficients, the error on a ratio of pumping power is calculated using the general uncertainty analysis. (Coleman et al., 2009) The ratio of scaled pumping power is

composed by a term of velocity, and the velocity can be converted into a term of heat transfer coefficient. The error of Kays and Crawfold heat transfer coefficient is between -2.5% and +11.1%. Error analysis is described in below.

The scaled pumping power is composed of the heat transfer coefficient terms as:

$$FOM_P \sim U^{2.75} = (h^{1.25})^{2.75} = h^{3.44} . \tag{4.33}$$

And also the ratio of scaled pumping power can be described using the heat transfer coefficient term.

$$S_P = \frac{FOM_{mix}}{FOM_{ref}} = \frac{h_{mix}^{3.44}}{h_{ref}^{3.44}} . \tag{4.34}$$

An error on the ratio of scaled pumping power is expressed by the general uncertainty analysis as:

$$(\varepsilon_{S_P})^2 = (\frac{\partial S_P}{\partial h_{mix}} \cdot \varepsilon_{h_{mix}})^2 + (\frac{\partial S_P}{\partial h_{ref}} \cdot \varepsilon_{h_{ref}})^2 , \tag{4.35}$$

$$(\varepsilon_{S_P})^2 = (3.44 \frac{h_{mix}^{2.44}}{h_{ref}^{3.44}} \cdot \varepsilon_{h_{mix}})^2 + (-3.44 \frac{h_{mix}^{3.44}}{h_{ref}^{4.44}} \cdot \varepsilon_{h_{ref}})^2 . \tag{4.36}$$

The error on the ratio of scaled pumping power can be written in terms of the error of the heat transfer coefficients as:

$$\frac{\varepsilon_{S_P}}{S_P} = \sqrt{(3.44 \frac{\varepsilon_{h_{mix}}}{h_{mix}})^2 + (-3.44 \frac{\varepsilon_{h_{ref}}}{h_{ref}})^2} . \tag{4.37}$$

The error of that is 39.14% as depicted in Fig. 4.18. The results show that the validation results using CFD code are within the error bar of scaled pumping power.

To confirm the boundary condition of developed correlation, the validation that carbon dioxide is selected as a reference gas is conducted. The results are

illustrated in Fig. 4.19. The result shows that the validation data is not in a good agreement with correlation using carbon dioxide as a reference case. This means that mixture gas which is only based on helium can be analyzed by developed correlation. However, The correlation show good agreement with the helium based region under 0.5 mole fraction of carbon dioxide which is additive component. This means that estimation in terms of developed correlation is available in helium based mixture gas region.

Table 4.1 Validation case

Mole fraction	
He	CO_2
1	0
0.9	0.1
0.8	0.2
0.7	0.3
0.6	0.4
0.5	0.5
0.4	0.6
0.3	0.7
0.2	0.8
0.1	0.9
0	1

Table 4.2 Grid information for validation (Lee, 2006)

Components		Number of elements
First wall	Fluid	1,080,800
	Structure	722,131
Breeding Zone	Fluid	1,275,359
	Structure	502,709

Table 4.3 Major design parameter of HCML TBM (Lee, 2006)

Design parameter	
Structural material	Eurofer
Coolant	He
Reflector	Graphite
Surface heat flux (average, peak) [MW/m^2]	0.3, 0.5
Neutron wall loading [MW/m^2]	0.78
First wall area [m^2]	0.719
Heat deposition (at avg. SHF) [MW]	0.675
Local TBR	0.276
Coolant inlet temperature, [℃] First wall Breeding zone	 300 361
Cooling system pressure [MPa]	8.0
Coolant mass flow rate [kg/s]	1.22

Table 4.1 CFX results for validation

He/CO_2 Mixture (700 K, 8 MPa)									
Fluid Condition			Maximum Temperature						Ratio of pumping power
Mole fraction		Velocity	Top			Bottom			CFX
He	CO_2		Line 1	Line 2	Line 3	Line 4	Line 5	Line 6	S_{Pump}
1	0	1	427.53	534.48	437.37	440.13	541.06	457.00	1
0.9	0.1	0.55	426.68	533.64	436.76	438.92	540.06	455.82	0.3375
0.8	0.2	0.4	427.36	533.95	437.47	439.51	540.37	456.33	0.1933
0.7	0.3	0.33	427.99	534.45	438.15	440.14	540.89	457.01	0.1427
0.6	0.4	0.3	427.79	534.21	438.15	439.71	540.57	456.64	0.1310
0.5	0.5	0.28	428.94	535.12	439.34	440.91	541.53	457.89	0.1254
0.4	0.6	0.28	429.17	535.21	439.76	440.94	541.57	457.98	0.1422
0.3	0.7	0.3	428.41	534.45	439.36	439.71	540.63	456.86	0.1924
0.2	0.8	0.33	428.80	534.66	440.05	439.84	540.77	457.09	0.2775
0.1	0.9	0.4	427.97	534.07	439.64	438.62	540.02	456.12	0.5203
0	1	0.52	428.61	534.36	440.78	438.82	540.19	456.47	1.1840

Table 4.5 Validation data of figure-of-merits (FOM)

He/CO_2 Mixture (700 K, 8 MPa)											
Mole fraction		Material properties				FOM		S_U		S_{Pump}	
X_{He}	X_{CO2}	ρ	C_P	μ	k	FOM_U	FOM_P	Correlation	CFX	Correlation	CFX
1	0	5.426	5.188	3.602.E-05	0.2852	3.935.E-05	2.113E-13	1	1	1	1
0.9	0.1	10.93	4.786	3.498.E-05	0.2618	2.138.E-05	6.622E-14	0.5433	0.55	0.3134	0.3375
0.8	0.2	16.43	4.384	3.428.E-05	0.2383	1.578.E-05	3.878E-14	0.4010	0.4	0.1835	0.1933
0.7	0.3	21.93	3.982	3.377.E-05	0.2149	1.330.E-05	3.000E-14	0.3380	0.33	0.1420	0.1427
0.6	0.4	27.43	3.58	3.338.E-05	0.1915	1.216.E-05	2.762E-14	0.3090	0.3	0.1307	0.1310
0.5	0.5	32.93	3.178	3.307.E-05	0.1681	1.180.E-05	2.909E-14	0.2999	0.28	0.1377	0.1254
0.4	0.6	38.44	2.776	3.283.E-05	0.1447	1.206.E-05	3.461E-14	0.3065	0.28	0.1638	0.1422
0.3	0.7	43.94	2.374	3.263.E-05	0.1213	1.298.E-05	4.676E-14	0.3299	0.3	0.2213	0.1924
0.2	0.8	49.44	1.972	3.246.E-05	0.09789	1.483.E-05	7.352E-14	0.3769	0.33	0.3479	0.2775
0.1	0.9	54.94	1.57	3.231.E-05	0.07448	1.832.E-05	1.420E-13	0.4656	0.4	0.6720	0.5203
0	1	60.44	1.168	3.219.E-05	0.05107	2.557.E-05	3.811E-13	0.6498	0.52	1.8036	1.1840

Table 4.6 RMS error of CFX calculation

He/CO_2 Mixture (700 K, 8 MPa)									
Fluid Condition			Temperature difference						RMS Error
Mole fraction		Velocity	Top			Bottom			
He	CO_2		Line 1	Line 2	Line 3	Line 4	Line 5	Line 6	
1	0	1	0.000	0.000	0.000	0.000	0.000	0.000	0.000
0.9	0.1	0.55	0.841	0.835	0.612	1.211	0.995	1.175	0.468
0.8	0.2	0.4	0.170	0.523	-0.097	0.623	0.688	0.661	0.134
0.7	0.3	0.33	-0.463	0.024	-0.783	-0.005	0.168	-0.014	0.071
0.6	0.4	0.3	-0.265	0.264	-0.776	0.424	0.490	0.357	0.107
0.5	0.5	0.28	-1.418	-0.641	-1.965	-0.781	-0.474	-0.895	0.660
0.4	0.6	0.28	-1.641	-0.734	-2.389	-0.803	-0.511	-0.990	0.902
0.3	0.7	0.3	-0.880	0.027	-1.994	0.420	0.426	0.137	0.427
0.2	0.8	0.33	-1.276	-0.180	-2.679	0.288	0.290	-0.099	0.752
0.1	0.9	0.4	-0.449	0.408	-2.270	1.510	1.035	0.877	0.803
0	1	0.52	-1.088	0.113	-3.405	1.316	0.862	0.529	1.296

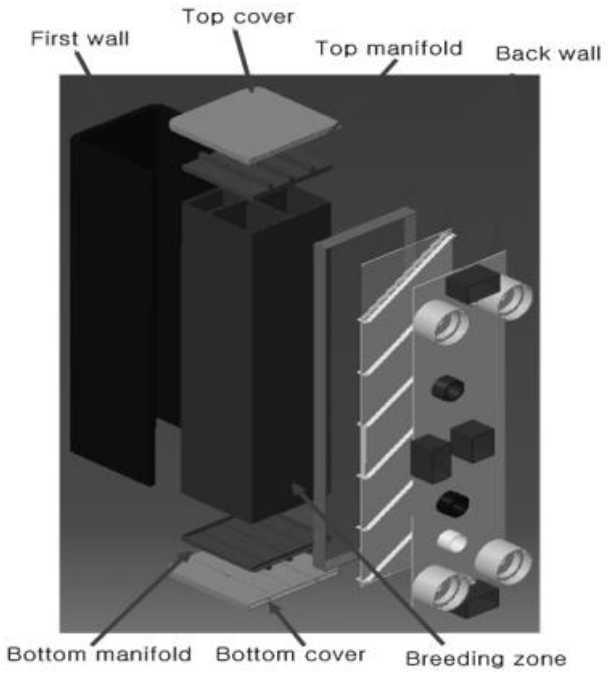

Figure 4.1 Schematic view of HCML TBM (Lee, 2006)

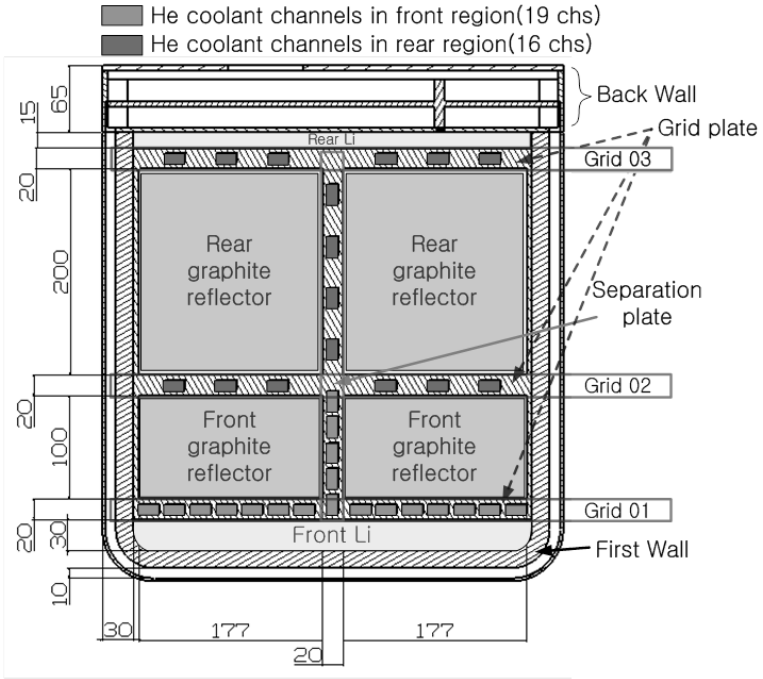

Figure 4.2 Cross-sectional view of HCML TBM (Lee, 2006)

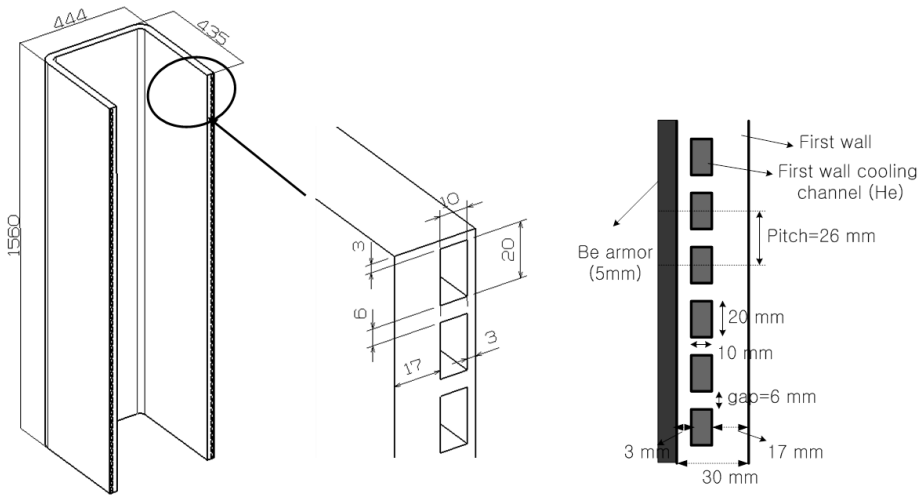

Figure 4.3 First wall channel size of HCML TBM (Lee, 2006)

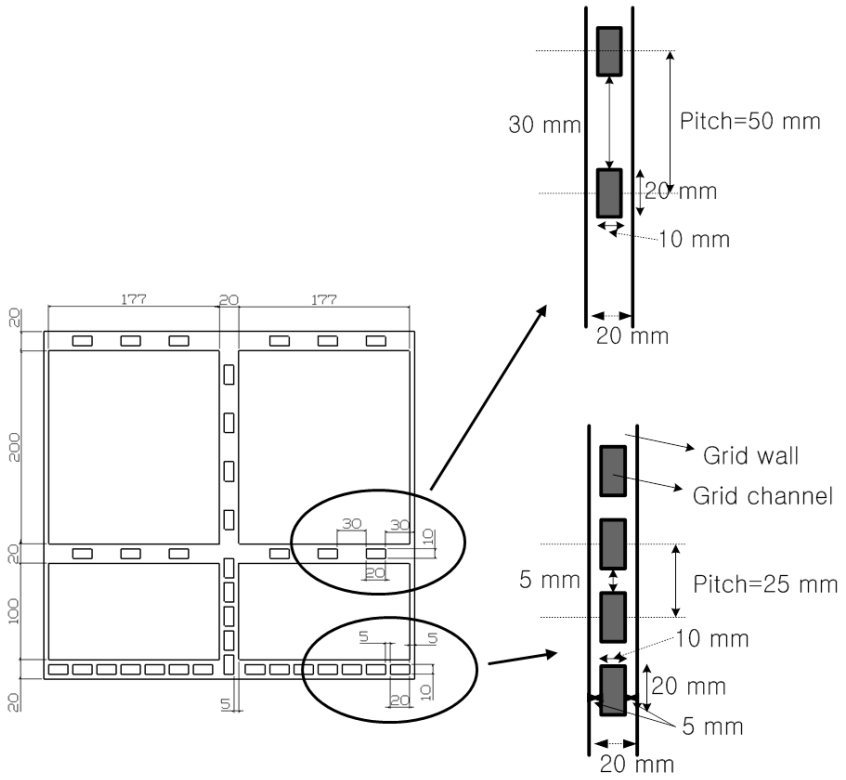

Figure 4.4 Breeding zone channel size of HCML TBM (Lee, 2006)

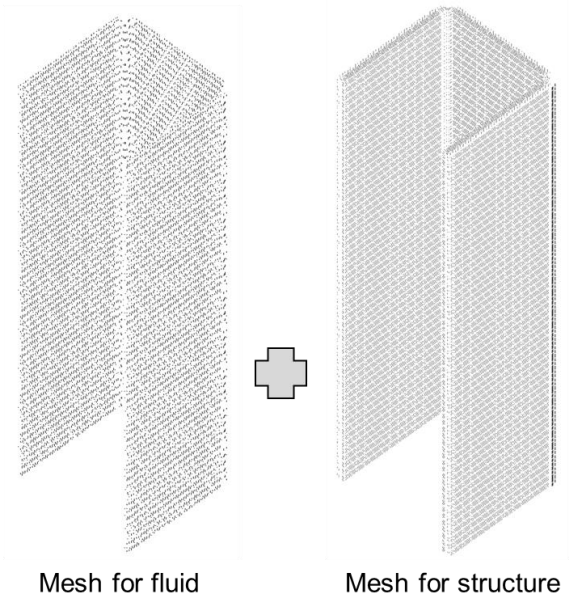

Figure 4.5 First wall mesh grid HCML TBM (Lee, 2006)

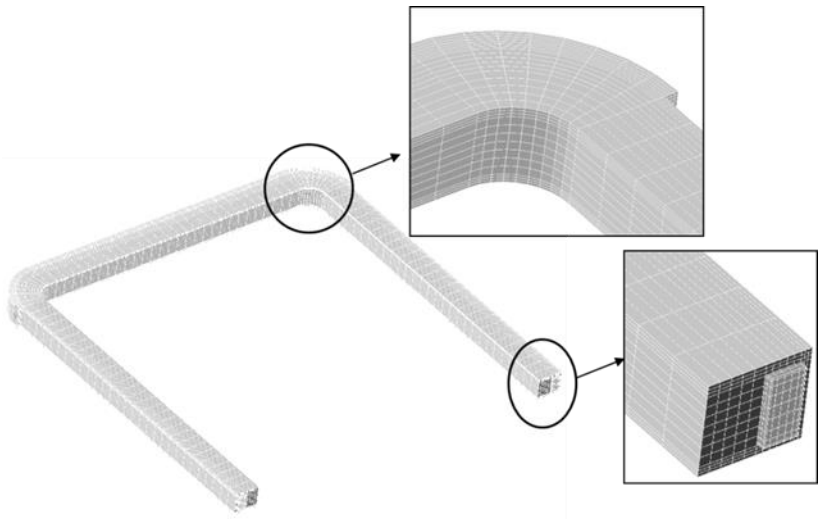

Figure 4.6 Single first wall channel mesh grid of HCML TBM (Lee, 2006)

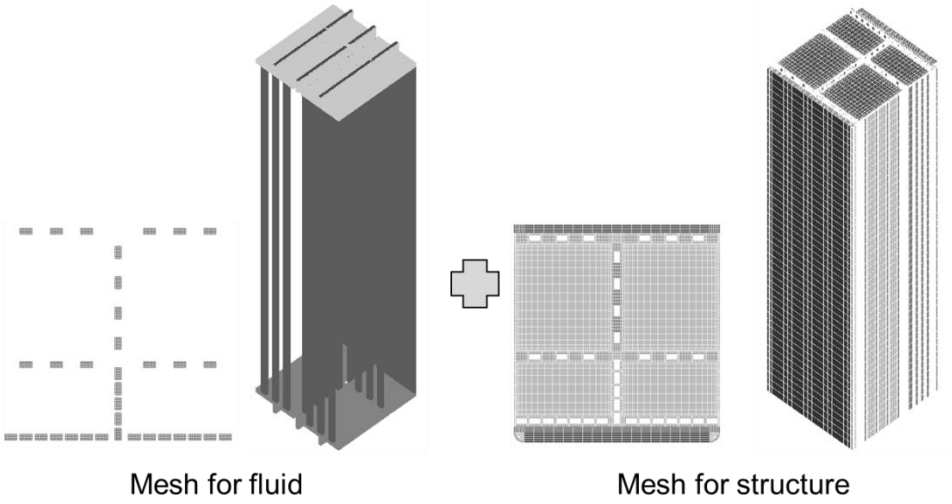

Figure 4.7 Breeding zone mesh grid HCML TBM (Lee, 2006)

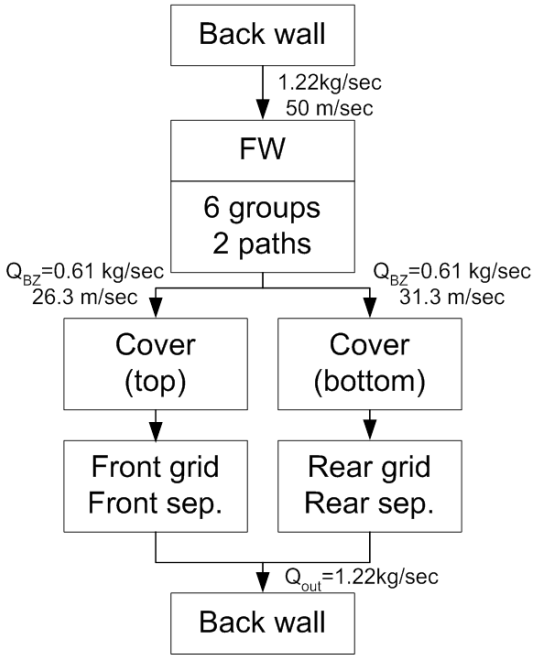

Figure 4.8 Helium flow in HCML TBM (Lee, 2006)

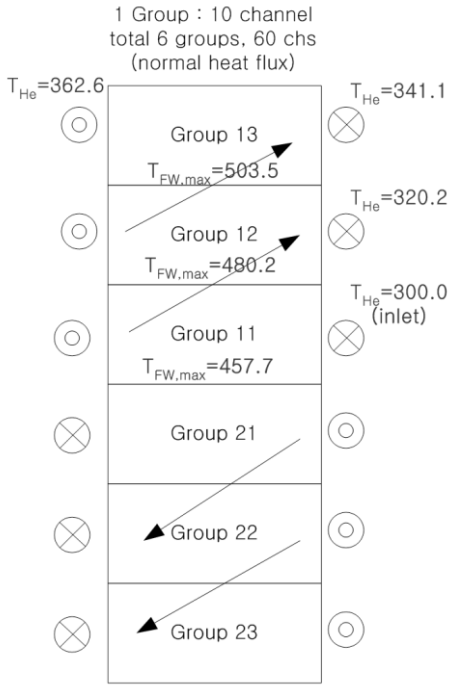

Figure 4.9 Inlet temperature of helium coolant HCML TBM (Lee, 2006)

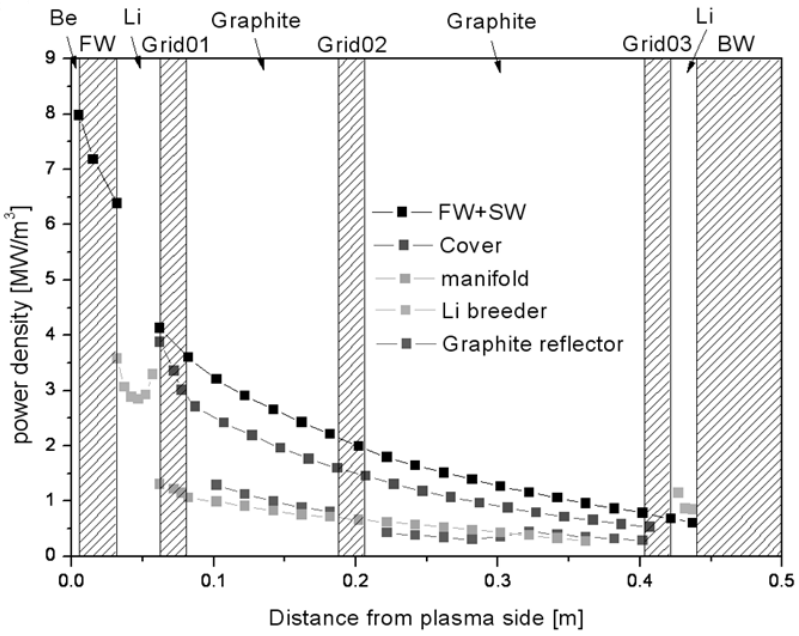

Figure 4.10 Neutron heat source in HCML TBM (Lee, 2006)

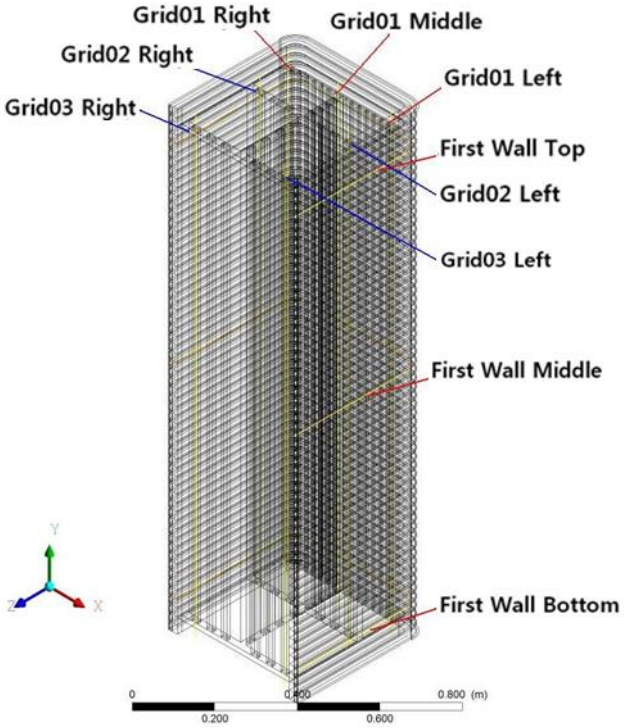

Figure 4.11 Grid line for validation (isometric view)

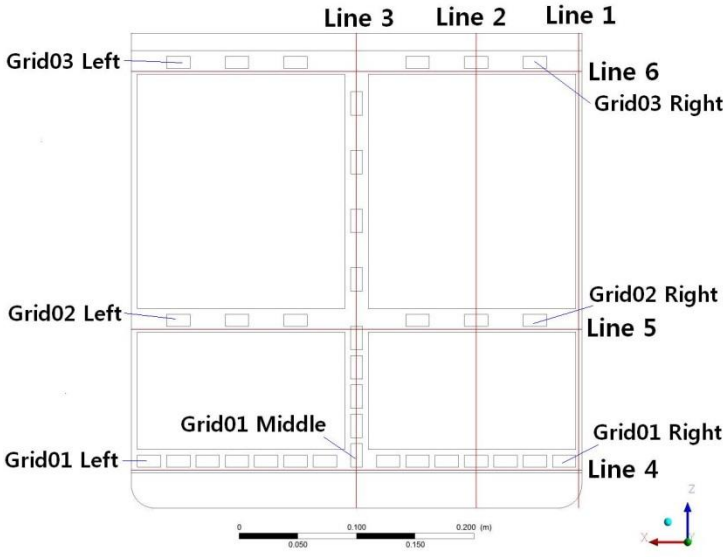

Figure 4.12 Grid line for validation (top view)

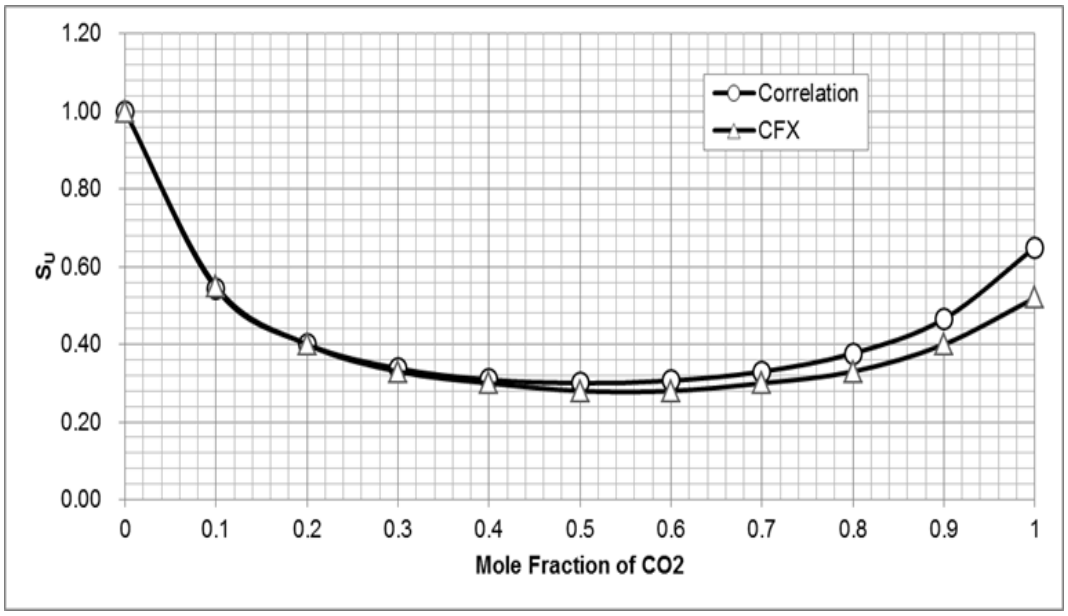

Figure 4.13 Validation results of scaled velocity

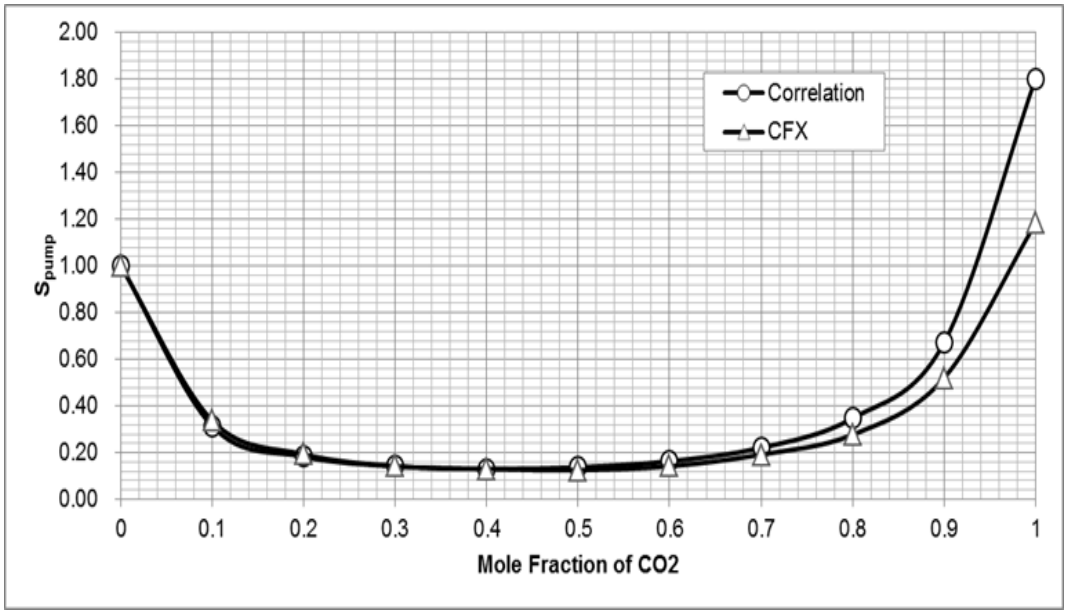

Figure 4.14 Validation results of scaled pumping power

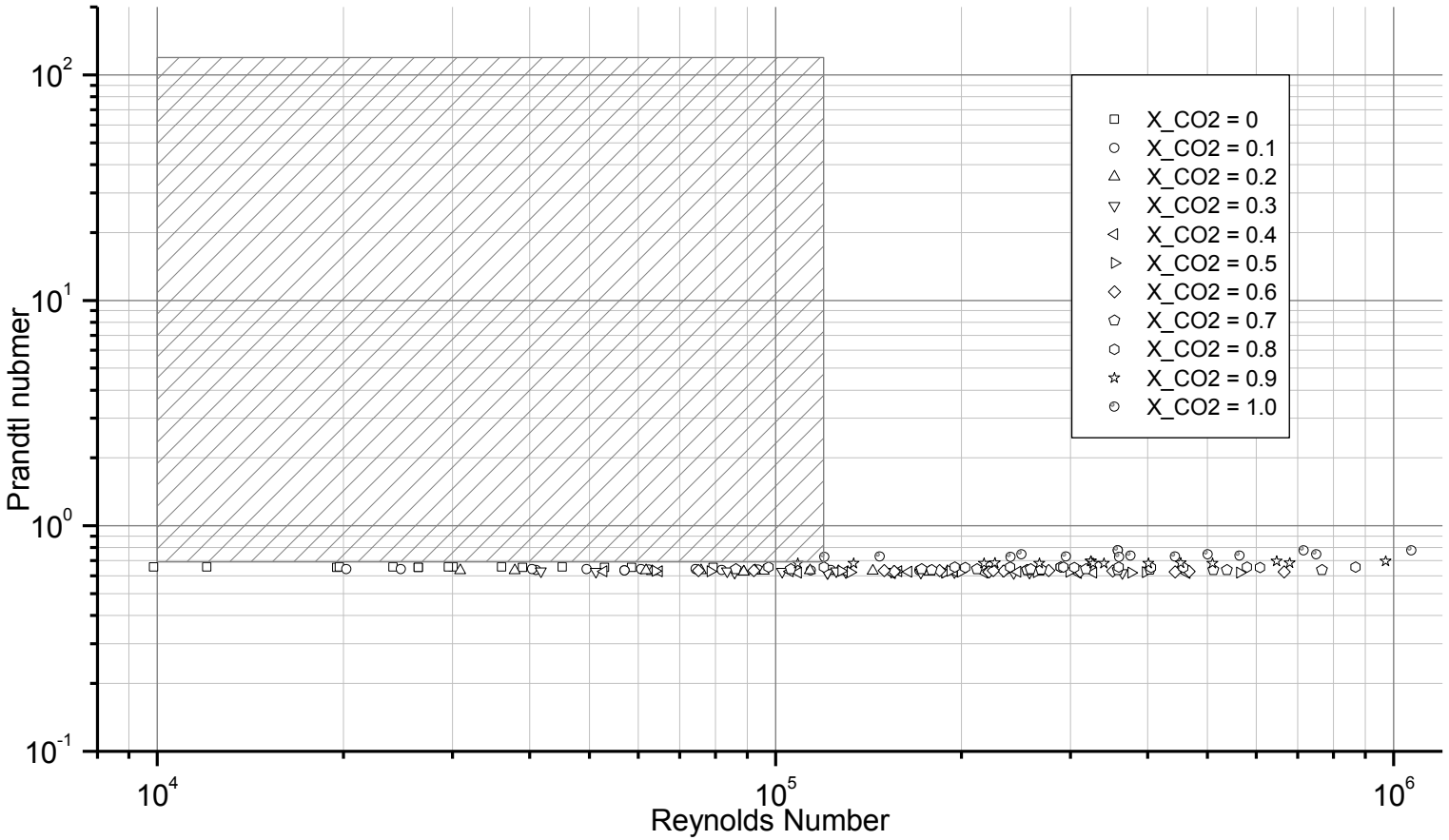

Figure 4.15 Range of Re and Pr number using Dittus-Boelter correlation with calculation data

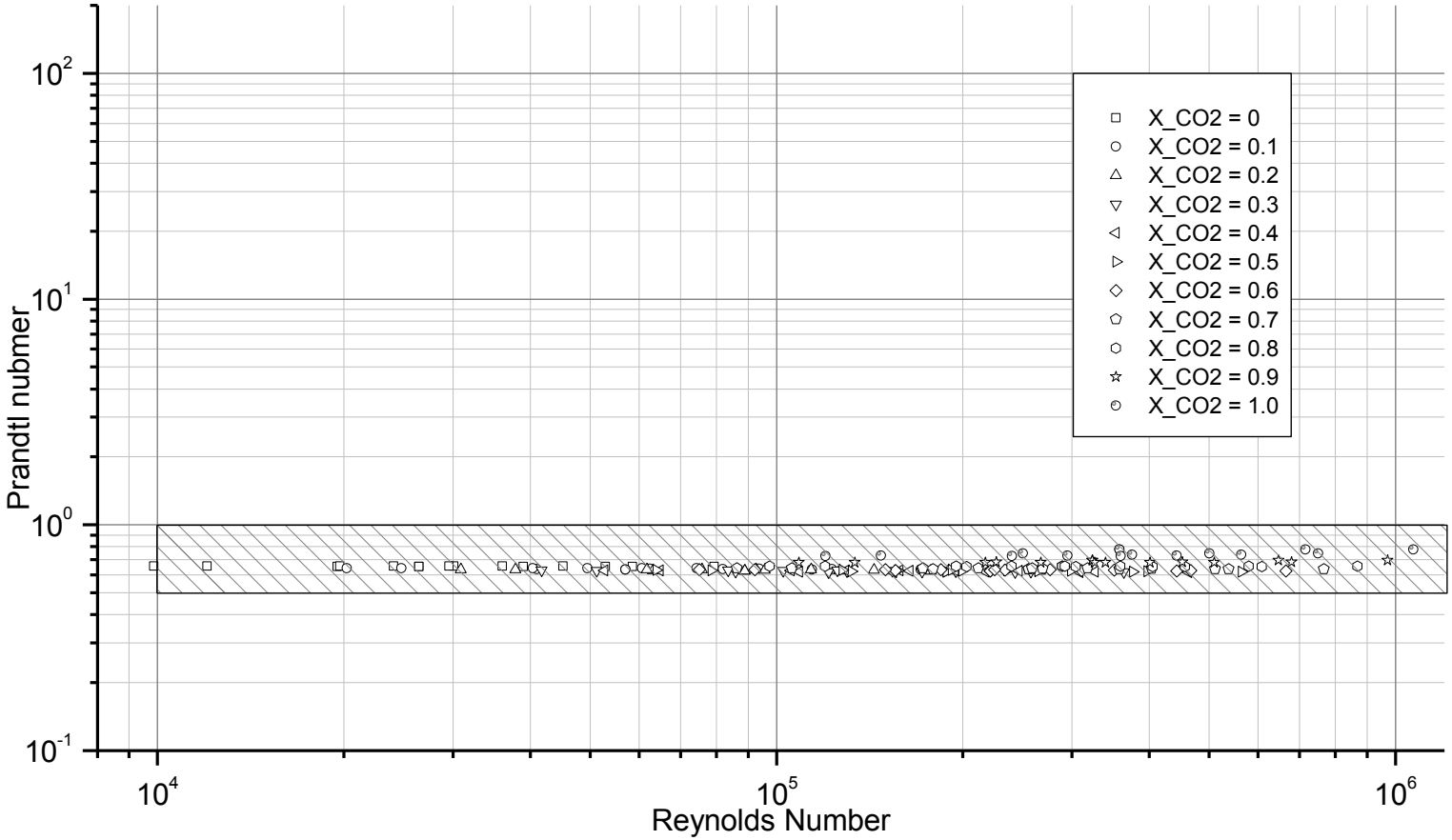

Figure 4.16 Range of Re and Pr number using Kays and Crawfold correlation with calculation data

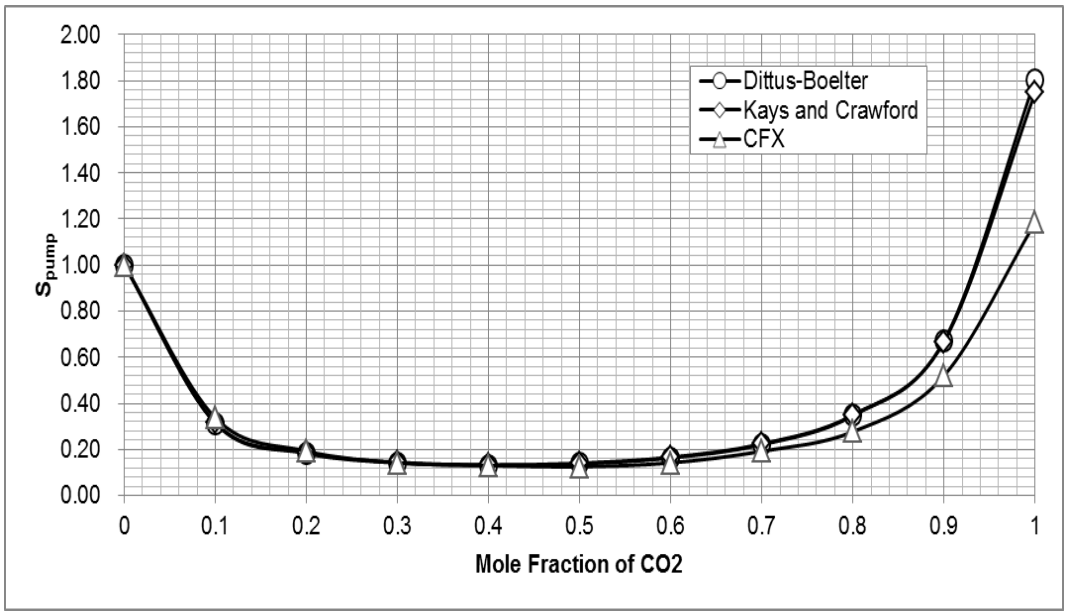

Figure 4.17 Validation results of scaled pumping power with Kays Crawfold correlation

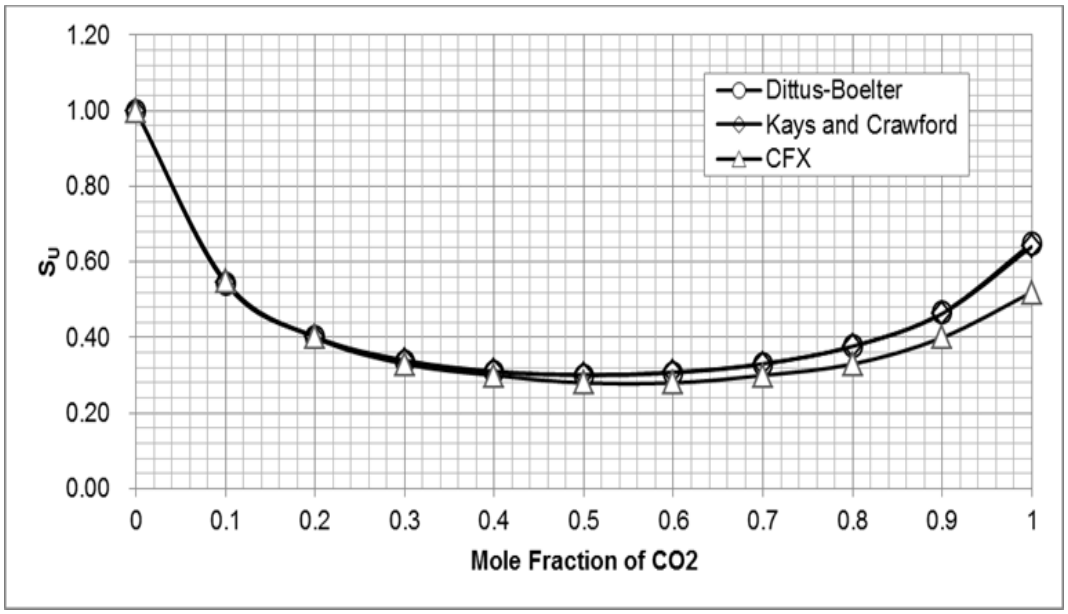

Figure 4.18 Validation results of scaled velocity with Kays Crawfold correlation

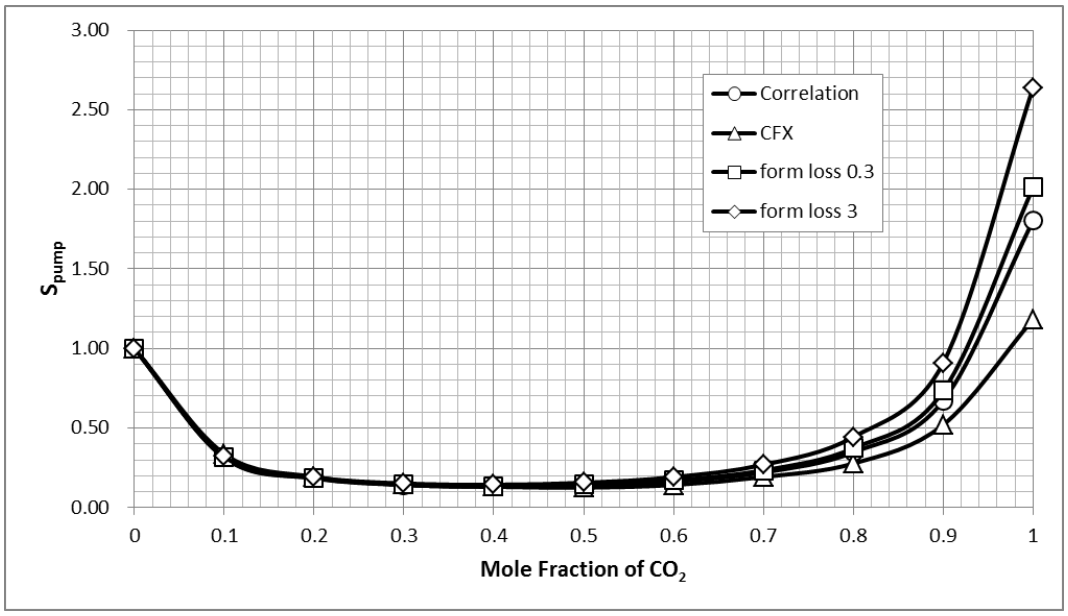

Figure 4.19 Validation results considering form loss

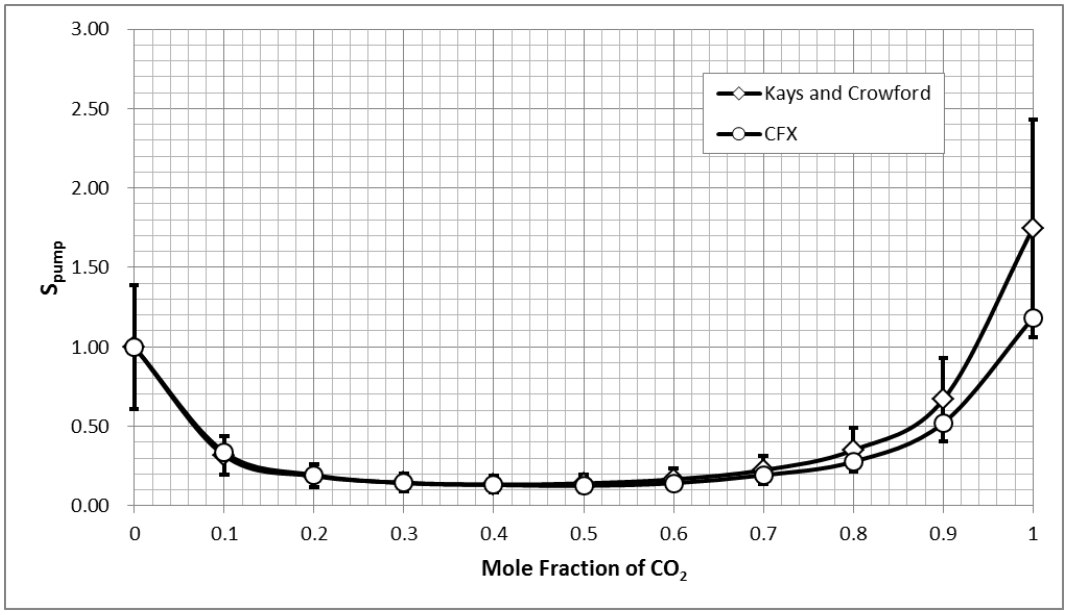

Figure 4.20 Error of scaled pumping power with Kays and Crawfold correlation

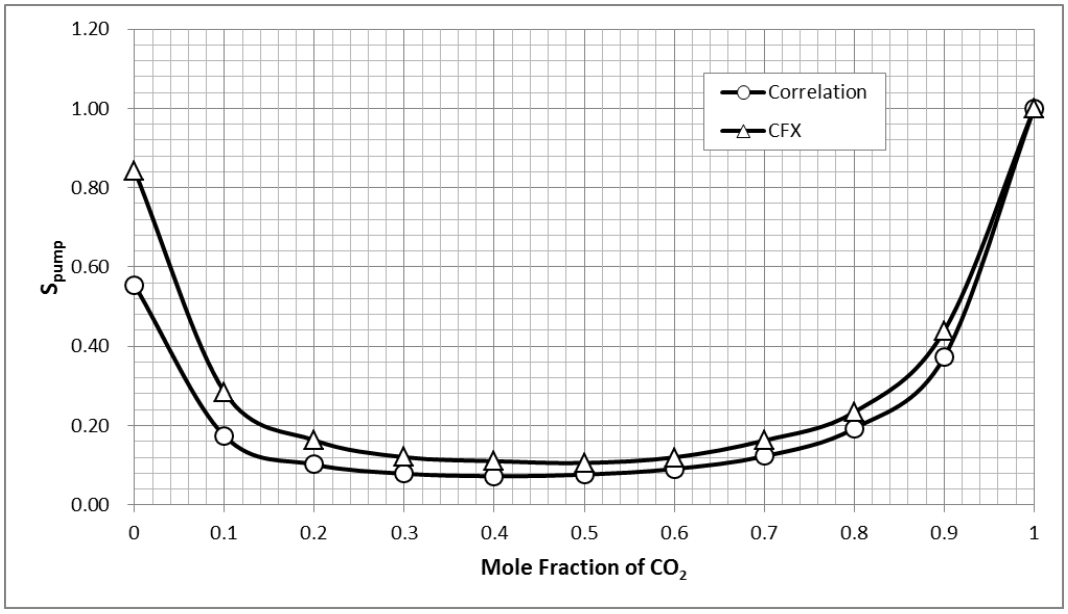

Figure 4.21 Validation results using carbon dioxide as reference gas

Chapter 5

Summary and Conclusion

To compare heat transfer performance of various gases and gas mixtures, the correlation for scaled velocity and the scaled pumping power are developed as a form of figure-of-merit (FOM). This means that the correlation can estimate relative velocity and pumping power for achieving the same heat transfer performance. Also, the correlations are only composed by four terms of material properties and two terms of overall geometry. This simple form of correlation makes estimation of the heat transfer performance of coolants convenient. So, the developed correlation can be utilized to check the cooling performance of various gases and mixtures before designing the blanket in details.

Validation for developed correlation is conducted on gas mixture, which is composed by helium and carbon dioxide. HCML TBM is selected for the validation model. This is because HCML TBM has general features of fusion blanket. The validation data which is calculated using Computational Fluid Dynamics code are in good agreement with the developed correlation in helium based gas mixture region. Furthermore, The sensitivities of Reynolds number and Prandtl number are tested, and the error of developed correlation is analyzed.

The evaluation results using developed correlation show that the binary gas mixture has improved heat transfer performance. By using xenon as a mixed gas,

only 4% of pumping power is needed when compared to pure helium coolant. And also, by using carbon dioxide and argon as mixed gas, which are easy to find, 13% and 26% of pumping power are needed comparing with pure helium coolant of that. Furthermore, the mechanism for enhancement of heat transfer performance of mixture gas is explained using the sensitivity of material properties for the scaled pumping power. However, there is no advantage of ternary gas mixtures in the heat transfer enhancement aspect. This can be explained that the optimum point is located on the binary gas mixture region. Moreover, the characteristics of the mixture properties model can be one of the reason why heat transfer performance cannot be improved using them.

The mixture gas concept for nuclear fusion blanket is proposed in this study. The gas mixture has better cooling performance compare to the pure helium gas and has certain the merits in terms of safety and leakage issues due to low operating pressure. These benefits of mixture gas concept are considered useful for designing the fusion blanket. This is because better heat transfer capacity of gas mixture concept is beneficial for designing the blanket in aspect of temperature window of structure material. Moreover, gas mixture concept has merit for reducing pumping power in the blanket. Thus, that concept can improve the efficiency of power conversion system.

Nomenclature

Symbols

Cp	:	heat capacity (J kg^{-1} K^{-1})
D	:	diameter (m)
FOM	:	figure-of-merit
G	:	volumetric flow rate (m^3 s^{-1})
h	:	heat transfer coefficient (W $m^{-2}K^{-1}$)
K	:	form loss coefficient
k	:	thermal conductivity (W m-1K^{-1})
L	:	length (m)
M	:	molecular weight (kg)
$\dot{m}$	:	mass flow rate (kg s^{-1})
P	:	power (W)
p	:	pressure (Pa)
Pr	:	Prandtl number
$\dot{Q}$	:	heat removal rate (W m^{-3})
Re	:	Reynolds number
S	:	ratio of figure-of-merit
T	:	temperature (K)
U	:	velocity (m s^{-1})
V	:	volume (m^3)
X	:	mole fraction

Greek symbols

α	:	Porosity
ε	:	Error
η	:	pump efficiency
μ	:	viscosity (kg $s^{-1}m^{-1}$)
ρ	:	density (kg m^{-3})

Subscript

0	:	reference case indicator
Cp	:	heat capacity indicator
eff	:	effective indicator
k	:	thermal conductivity indicator
K		form loss indicator
Kays		Kays Crawfold correlation indicator
mix	:	mixture case indicator
P	:	pumping power indicator
pump	:	pump indicator
ref	:	reference case indicator
U	:	velocity indicator
μ	:	viscosity indicator
ρ	:	density indicator

References

ANSYS, INC. "ANSYS-CFX Solver Theory Guide," ANSYS CFX Release 11, 2010.

Blasius, H., "Das Aehnlichkeitsgesetz bei Reibungsvorgängen in Flüssigkeiten," *Mitteilungen über Forschungsarbeiten auf dem Gebiete des Ingenieurwesens*, vol.131, VDI-Verlag Berlin., 1913.

Coleman, H. W., and Steele, W. G., "Experimentation, validation, and uncertainty analysis for engineers," John Wiley & Sons, 2009.

Davidson, T. A., "A simple and accurate method for calculating viscosity of gaseous mixtures," 1993.

Dittus, F. W. and Boelter, L. M. K., "University of California Publications on Engineering," University of California Publications in Engineering., 1930.

El-Genk, M. S., and Tournier, J.M., "On the use of noble gases and binary mixtures as reactor coolants and CBC working fluids," *Energy Conversion and Management*, vol.49(7), pp. 1882-1891, 2008.

Enoeda, M., Kosaku, Y., Hatano, T., Kuroda, T., Miki, N., Honma, T., ... & Okano, K., "Design and technology development of solid breeder blanket cooled by supercritical water in Japan," *Nuclear fusion*, vol.43(12), 1837., 2003.

Graham, T., "On the motion of gases," Philosophical Transactions of the Royal Society of London 136, pp. 573-631, 1846.

Herning, F., and Zipperer, L., "Calculation of the viscosity of technical gas mixtures from the viscosity of individual gases," Gas u, Wasserfach, 1936.

ITER, E., "Final Design Report," ITER Technical Basis, Plant Description

Document (PDD), G A0 FDR, 1, 01-07., 1998.

Kakaç, S., Shah, R. K., & Aung, W., eds. “Handbook of single-phase convective heat transfer,” New York et al., Wiley, 1987.

Kays, W. M., Crawford, M. E. and Weigand, B., “Convective heat and mass transfer,” McGraw-Hill Higher Education, 2005.

Kim, K., Kim, H. C., Oh, S., Lee, Y. S., Yeom, J. H., Im, K., ... & Titus, P., “A preliminary conceptual design study for Korean fusion DEMO reactor,” *Fusion Engineering and Design*, 2013.

Klein, S. A., and Alvarado, F. L., "Engineering equation solver," F-Chart Software, Box 44042, 2002.

Lee, D. W., “HCML Design,” KAERI TBM Team, 2006.

Lee, D. W., Hong, B. G., Kim, S. K. and Kim, Y., “Design and preliminary safety analysis of a helium cooled molten lithium test blanket module for the ITER in Korea,” *Fusion Engineering and Design*, vol. 83, pp. 1217-1221, 2008.

Lee, D. W., Hong, B. G., Kim, Y., In, W. K., Yoon, K. H., “Helium cooled molten lithium TBM for the ITER in Korea,” *Fusion Science and Technology*, vol.52, pp. 844-848, 2007

Lee, D. W., Hong, B. G., Kim, Y., In, W. K., Yoon, K. H., “Preliminary design of a helium cooled molten lithium test blanket module for the ITER test in Korea,” *Fusion Engineering and Design*, vol.82, pp. 381-388, 2007

Lee, D.W., Hong, B.G., Song, K.W., Kim, Y.H., Song, G.N., In, W.G. and Yoon, K.H., “Current status and R & D plan on ITER TBMs of Korea,” *Journal of the Korean Physical Society*, Vol.49, pp.S340-S344, 2006.

Lee, G. S., Kwon, M., Doh, C. J., Hong, B. G., Kim, K., Cho, M. H., ... & Chang, H. Y., “Design and construction of the KSTAR tokamak,” *Nuclear Fusion*, 41,

1515, 2001.

Lemmon, E. W., Huber, M. L. and McLinden, M. O., "NIST reference fluid thermodynamic and transport properties-REFPROP," Physical and Chemical Properties Division, National Institute of Standards and Technology, Boulder, Colorado, 80305, 2007.

Lienhard, J. H., “A heat transfer textbook,” Courier Dover Publications, 2011.

McAdams, W. H., “Heat transmission,” Vol. 3. New York: McGraw-Hill, 1954.

Piet, S. J., Jeppson, D. W., Muhlestein, L. D., Kazimi, M. S., & Corradini, M. L., “Liquid metal chemical reaction safety in fusion facilities,” *Fusion engineering and design*, 5. 3, 273-298, 1987.

Reid, R. C., Prausnitz, J. M., and Poling, B. E., "The properties of gases and liquids,” 1987.

Tomabechi, K., Gilleland, J. R., Sokolov, Y. A., Toschi, R., & Team, I. T. E. R., “ITER conceptual design,” *Nuclear Fusion*, 31, 1135, 1991.

Wilke, C. R., "A viscosity equation for gas mixtures," *The Journal of Chemical Physics*, vol. 18, pp. 517, 1950.

Zinkle, S. J., and Ghoniem, N. M., “Operating temperature windows for fusion reactor structural materials,” *Fusion Engineering and design*, 51, 55-71, 2007

국문 초록

핵융합로 블랭킷 냉각재로써 헬륨은 안전성이 뛰어나다는 장점이 있지만 냉각능력이 떨어지는 문제점이 존재한다. 이러한 문제를 해결하기 위하여 본 연구는 헬륨의 안전성을 유지하며 냉각능력을 향상시키는 방법으로 혼합기체를 이용한 핵융합로 블랭킷 냉각 개념에 대한 내용을 다루었다.

본 연구에서는 동일한 열 제거 성능을 가지기 위한 냉각재의 상대적 속도와 펌핑파워를 예측하는 상관식을 개발하였다. 상관식은 네 개의 냉각재의 물성치와 두 개의 구조적 변수를 이용하여 계산할 수 있도록 개발하였다. 상관식 개발을 위하여 열전달계수와 마찰 계수로써 Dittus-Boelter 상관식과 Blasius 상관식을 사용하였다. 개발한 상관식은 핵융합로 블랭킷 상세설계 이전에 여러 기체 및 혼합기체의 냉각능력을 비교하는 데 사용할 수 있도록 개발되었다.

핵융합로 블랭킷 냉각재로서 혼합기체의 냉각능력 평가는 개발한 상관식을 기반으로 수행되었다. 냉각능력 평가를 위하여 헬륨과의 혼합기체로 이산화탄소, 알곤, 네온, 크립톤, 제논, 질소를 선정하였다. 평과 결과를 통하여 혼합기체 이용 시 냉각능력의 증진을 확인하였다. 또한, 혼합기체를 이용하여 냉각능력을 향상시키는 동시에 운전 압력을 낮춤으로써 안전성을 높이는 방안을 제안하였다. 그러나 세 가지 가스를 혼합기체로 이용할 경우 냉각 능력 증진 측면에서 이점이 없는 것을 확인하였다.

개발한 상관식은 전산유체역학 코드를 이용하여 검증을 수행하였다. 검증 모델로 ITER HCML TBM을 사용하였으며 헬륨과 이산화탄소의 혼합기체를 이용하여 검증을 수행하였다. 전산유체역학 코드를 이용한 검증 결과와 비교해 보았을 때 헬륨 기반의 혼합기체 영역에서 상관식이 잘 일치 하는 것을 확인하였다. 추가로 개발한 상관식의 예측능력 향상을 위하여 레이놀즈 수와 프란틀 수를 확인하였으며 개발한 상관식에 Kays and Crawfold 열전달 상관식을 적용해 보았다. 또한 열전달 상관식의 오차에 의한 상대적 속도 및 펌핑파워에 대한 상관식의 오차를 계산하였다.

주요어
기체 냉각 핵융합로, 핵융합로 냉각재, 혼합 기체, 성능계수, 전산유체역학, ITER HCML TBM

학번: 2011-23422

감사의 글

스승으로써 많은 배움의 기회를 주시고 언제나 저에게 관심을 가져 주셨던 박군철 선생님께 진심으로 감사드립니다. 선생님의 제자로써 부끄럽지 않은 사람이 될 수 있도록 더 노력하겠습니다. 대학원에 입학할 때부터 저를 지켜봐 주시면서 성장할 수 있도록 도와주시고 연구에 흥미를 가질 수 있도록 일깨워 주신 김응수 교수님께 깊은 감사를 드립니다. 학위과정과 대학원 생활을 통하여 연구자의 태도에 대하여 진지하게 고민할 수 있도록 가르쳐 주신 조형규 교수님께 진심으로 감사를 드립니다. 대학원생인 저의 사소한 질문도 성심성의껏 답변해 주시고 핵융합 열수력 연구 분야에서 저에게 귀감이 되어주신 이동원 박사님께 깊은 감사를 드립니다. 더불어 제가 연구를 할 수 있도록 여러 방면에서 도와주신 핵융합 연구소의 김기만 박사님, 김형찬 박사님, 이영석 박사님, 임기학 박사님께 큰 감사를 드립니다. 열수력 연구실에서 핵융합에 관련된 일을 할 수 있도록 관심을 가지고 도와주셨던 나용수 교수님, 황용석 교수님, 한정훈 박사님께 진심으로 감사드립니다. 더불어 저를 지켜봐 주신 주한규 교수님과 김곤호 교수님 그리고 원자핵공학과 교수님들께 감사를 전하고 싶습니다.

제가 연구실에 입학하기 이전부터 저에 대하여 관심을 가지고 많은 조언을 해주신 종원이형과 수종이 형, 학업에 있어 많은 가르침을 주셨고 앞으로도 같이 일할 수 있는 기회가 있기를 바라는 연건이형, 학부생 때부터 실험에 관심을 가지게 해주신 거형이형, 실험장치를

같이 만들고 많은 고민을 나누면서 제 연구실 생활에 가장 긴 시간을 함께 한 진석이형, 가끔씩 오셔서 많은 조언을 해주시는 성수형, 연구실에서 많은 궂은일을 하느라 고생하신 태진이형, 항상 뭐든지 올바른 길을 보여주시고자 하셨던 정훈이형, 석사 생활에 도움을 주었던 지훈이형, 수빈누나, 연구실의 분위기를 고민하고 저에게 많은 생각을 할 수 있게 해주었던 룸메이트 진화형, 더불어 많은 연구실 선배님들께 진심으로 감사드립니다.

언제나 앞장서서 모범을 보이는 민섭이형과 재순이형, 후배로써 더 큰 모범을 보이는 세린이, 한심한 나랑 항상 잘 놀아주는 해윤이, 앞으로 들어올 제희와 상진이에게 큰 감사를 전합니다. 특히 박민영과 신동호님의 하해와 같은 가르침에 감사드립니다. 너희가 없었으면 연구실을 졸업할 수 없었을 거라고 생각하고 언제든 나를 부르면 부탁을 들으러 날아오도록 할게.

대학생활의 추억을 같이 한 권순우, 김상진, 네임드 박용택, 변철식, 손성준, 이현배, 인수교, 조덕현, 주희재 정신차리고 열심히 살았으면 좋겠고 앞으로 더 많은 추억을 만들자. 언제나 부족한 내 곁을 지켜준 예지에게 특별히 고맙다는 말을 남기며 앞으로 더 많이 행복한 시간을 보낼 수 있도록 노력할게.

이제는 많이 철이 들어 어느덧 대견스러워 보이는 내 동생 현웅이에게 고맙게 생각하고, 마지막으로 저를 있게 해주시고 저에게 헌신해 주신 그리고 언제나 저를 믿어주셨던 사랑하는 아버지와 사랑하는 어머니께 이 논문을 바칩니다.